The Dense-Core Vesicle Maturation Protein CCCP-1 Binds both RAB-2 and Membranes through a Conserved C-terminal Coiled-coil Domain

Jérôme Cattin-Ortolá[‡], Irini Topalidou[‡], Annie Dosey[‡], Alexey J. Merz[‡, §] and Michael Ailion[‡1]

From the [‡]Departments of Biochemistry and [§]Physiology and Biophysics, University of Washington, Seattle, WA, 98195 USA

Running title: Structure-function analysis of CCCP-1

[1]To whom correspondence should be addressed: Michael Ailion, Department of Biochemistry, University of Washington, Box 357350, 1705 NE Pacific St, Seattle, WA 98195, Tel: 206-685-0111, Fax: 206-685-1792, E-mail: mailion@uw.edu

Keywords: Membrane trafficking, dense-core vesicle, Rab, GTPase, *Caenorhabditis elegans*, coiled-coil domain, golgin, protein trafficking (Golgi), lipid binding protein

ABSTRACT

Dense-core vesicles (DCVs) are secretory organelles that store and release modulatory neurotransmitters from neurons and endocrine cells. Recently, the conserved coiled-coil protein CCCP-1 was identified as a component of the DCV biogenesis pathway in the nematode *C. elegans*. CCCP-1 binds the small GTPase RAB-2 and colocalizes with it at the trans-Golgi. Here we report a structure-function analysis of CCCP-1 to identify domains of the protein important for its localization, binding to RAB-2, and function in DCV biogenesis. We find that the CCCP-1 C-terminal domain (CC3) has multiple activities. CC3 is necessary and sufficient for CCCP-1 localization to the trans-Golgi and for binding to RAB-2, and is required for the function of CCCP-1 in DCV biogenesis. Additionally, CCCP-1 binds membranes directly through its CC3 domain, indicating that CC3 comprises a previously uncharacterized lipid-binding motif. We conclude that CCCP-1 is a coiled-coil protein that binds an activated Rab and localizes to the Golgi via its C-terminus, properties similar to members of the golgin family of proteins. Consistent with this idea, CCCP-1 also shares biophysical features with golgins.

Dense-core vesicles (DCVs)[2] are specialized organelles of neurons and endocrine cells. DCVs store and release modulatory peptides and biogenic amines, signaling molecules that control a multitude of processes including synaptic plasticity, feeding behavior, and glucose homeostasis (1–4). However, DCV biogenesis is not well understood, especially at the molecular level. Immature DCVs bud off from the trans-Golgi and undergo several maturation steps, including homotypic fusion with other immature DCVs, vesicle acidification, peptide processing, and sorting of cargos (1–4). In recent years, a small but growing number of proteins have been identified as playing roles in DCV biogenesis, beginning to shed some light on the molecular mechanisms underlying the steps in DCV maturation (5–18). In one approach to identifying proteins important for DCV biogenesis, genetic screens were performed in *Caenorhabditis elegans* (19–25). These screens identified several molecules important for early stages of DCV biogenesis and maturation, including the small G protein RAB-2 and several RAB-2 effectors, including the conserved coiled-coil protein CCCP-1 (24). Here we perform a structure-function analysis of CCCP-1 in order to better understand its biochemical activities and role in DCV biogenesis.

RAB-2 is a highly conserved member of the Rab family of small G proteins. Rabs are membrane-associated proteins that function as molecular switches that alternate between a GTP-bound active state and a GDP-bound inactive state (26). Activated Rabs recruit effectors that execute many aspects of membrane trafficking including

vesicle transport and vesicle tethering (26). CCCP-1 was recently identified as a new RAB-2 effector (24, 27). In *C. elegans*, RAB-2 and CCCP-1 colocalize near the trans-Golgi and function in the same genetic pathway to regulate locomotion and DCV cargo sorting in neurons (24). CCCP-1 is predicted to be a long coiled-coil protein (24, 27), structurally similar to a family of tethers called golgins that bind activated Rabs and regulate vesicular trafficking at the Golgi (28–32). The elongated shape of golgins makes them suitable to tether incoming vesicles and promote vesicle fusion (28–32). Though CCCP-1 is critical for proper DCV biogenesis, its specific molecular function remains unclear. Here we conduct a structure-function analysis to determine which domains of CCCP-1 are important for its localization, binding to RAB-2, and function in DCV biogenesis. We find that CCCP-1 has structural and functional features in common with the golgins, suggesting that it may act as a membrane tether.

RESULTS

CCCP-1 is localized via its C-terminal domain CC3—To assess the localization of full length CCCP-1 in *C. elegans* neurons, we generated transgenic worms expressing GFP-tagged CCCP-1. When expressed under its own promoter, either as a single-copy integration or as multiple copies in an extrachromosomal array, CCCP-1::GFP levels were too low to be detected in most transgenic lines. However, these constructs are functional since they rescued the locomotion defects of a *cccp-1* mutant (see below). Because CCCP-1 is expressed predominantly in *C. elegans* neurons (24), we expressed CCCP-1::GFP under the stronger pan-neuronal *rab-3* promoter. CCCP-1 localized mainly to perinuclear puncta in the soma of ventral cord motor neurons (Fig. 1A, top) but also localized to puncta in axons in the dorsal nerve cord (Fig. 1A, bottom), suggesting that some CCCP-1 is transported out of the cell body.

To determine which domain of CCCP-1 mediates its localization to membranes, we generated transgenic worm lines carrying different GFP-tagged CCCP-1 fragments (Fig. 1B) expressed under the pan-neuronal *rab-3* promoter. Like full-length CCCP-1::GFP, CC2+3::GFP and CC3::GFP localized to perinuclear puncta (Fig. 1C). CC2+3::GFP also localized to a number of smaller puncta, but CCCP-1::GFP and CC3::GFP localized mostly to larger puncta. Like CCCP-1::GFP, CC2+3::GFP and CC3::GFP had puncta in the dorsal nerve cord as well (data not shown). In contrast, CC1+2::GFP was localized diffusely in the cytoplasm (Fig. 1C) as well as in the dorsal nerve cord (data not shown). These results are consistent with data showing that the N-terminal half of human CCCP1/CCDC186 localized to the cytosol and a C-terminal fragment larger than CC3 localized to perinuclear structures in COS cells (27). Our data indicate that the C-terminal domain CC3 is both necessary and sufficient for CCCP-1 localization to perinuclear puncta.

To test whether CC3 is also sufficient for localization of mammalian CCCP1/CCDC186 to the trans-Golgi, we imaged GFP-tagged rat CCCP1/CCDC186 and CCCP1/CCDC186 fragments in rat insulinoma 832/13 cells (33). These cells have secretory granules similar to DCVs, and express the mammalian ortholog of CCCP-1, CCCP1/CCDC186 (25). We found that full length CCCP1::GFP localizes to perinuclear puncta that partially overlap with the trans-Golgi marker TGN38 (Fig. 2A). Thus, as in *C. elegans* neurons and COS cells (24, 27), CCCP1 localizes to the trans-Golgi in 832/13 cells. CC1+2 localizes to the cytoplasm in 832/13 cells (Fig. 2B) and CC3 localizes to perinuclear puncta that partially overlap with TGN38 (Fig. 2C), consistent with our results in *C. elegans*. We conclude that CC3 is necessary and sufficient for CCCP1/CCDC186 localization to the trans-Golgi.

CCCP-1 binds RAB-2 via its C-terminal CC3 domain—Multiple lines of evidence suggest that CCCP-1 is an effector of the small GTPase RAB-2. CCCP-1 and RAB-2 act in the same genetic pathway in *C. elegans* and they colocalize in worm neurons and in COS cells (24, 27). In addition, yeast two-hybrid experiments showed that the CCCP-1 and RAB-2 proteins, from either worm or human, interact directly in a GTP-dependent manner (24, 27). The interaction of human CCCP1/CCDC186 with human RAB2 was mapped down to the CCCP1/CCDC186 C-terminus (27). To confirm the RAB-2 interaction with CCCP-1 using bacterially-expressed purified *C. elegans* proteins, we performed GST pull-downs and found that CCCP-1 binds to RAB-2 loaded with the non-hydrolysable GTP analog

guanosine 5'-O-[gamma-thio]-triphosphate (GTPγS, Fig. 3, lane 1), but not to RAB-2 loaded with GDP (Fig. 3, lane 2). The interaction of CCCP-1 with RAB-2 could be detected only by using an antibody to the His_6 epitope tag, indicating that the interaction is likely of moderate affinity.

To determine what domain of CCCP-1 binds to RAB-2, we performed GST pull-down experiments using the CCCP-1 fragments. CC2+3 and CC3, but not CC1+2, bound to RAB-2 in a GTP-dependent manner (Fig. 3), demonstrating that CC3 is necessary and sufficient for RAB-2 binding.

In *C. elegans*, CCCP-1 localizes to perinuclear puncta in the absence of RAB-2 (24), indicating that RAB-2 is not the sole determinant of CCCP-1 localization. We found that the localization of CC2+3 and CC3 is also unaltered in the absence of RAB-2 (Fig. 1C). Thus, the CC3 domain has at least two independent activities: RAB-2 binding and subcellular targeting.

CC3 is necessary for CCCP-1 function—To test whether CC3 is sufficient for the in vivo neuronal function of CCCP-1, we assayed CCCP-1 function in *C. elegans*. *cccp-1* mutant worms have a slow locomotion phenotype (24). Because overexpression of CCCP-1 also causes slow locomotion, we made single-copy integrants of transgenes expressing the different CCCP-1 fragments under the endogenous *cccp-1* promoter, and tested for rescue of the *cccp-1* mutant slow locomotion phenotype. Expression of full-length CCCP-1 rescued the locomotion defect of *cccp-1* mutants (Fig. 4A), but neither CC1+2 nor CC3 rescued (Fig. 4B). Thus, CC3 is necessary but not sufficient for CCCP-1 function.

CCCP-1 binds membranes directly— The colocalization of CCCP-1 puncta with RAB-2 and trans-Golgi markers suggests that CCCP-1 may be localized to a membrane compartment, but CCCP-1 does not have a predicted transmembrane domain. To test whether CCCP-1 is a cytosolic protein associated with membranes, we used the rat insulinoma 832/13 cell line (33). We transfected cells with a construct expressing GFP-tagged rat CCCP1/CCDC186 and performed membrane fractionation assays (Fig. 5A). Most of the CCCP1/CCDC186 protein associated with membranes (Fig. 5A, P90 membrane pellet versus S90 soluble fraction). In the presence of either 1 M NaCl or 1% Triton X-100, CCCP1/CCDC186 was soluble. CCCP1/CCDC186 therefore behaves as a peripheral membrane protein.

Membrane association of CCCP-1 could occur via binding an additional protein or through its direct interaction with the phospholipid bilayer. We assayed whether the purified CCCP-1 protein binds lipids directly in blot overlay and liposome flotation experiments. We generated liposomes containing cholesterol and lipids with neutral and charged head groups that mimic the lipid composition of the Golgi (34). The liposomes were doped with a fluorescent lipid, rhodamine-phosphatidylethanolamine (Rh-PE). We incubated liposomes and protein at the bottom of a stepped sucrose density gradient (Fig. 5B). When centrifuged, most of the Rh-PE-labeled liposomes floated to near the top of the gradient, and most of the CCCP-1 protein migrated with the liposomes (Fig. 5C, lanes 4 and 5). In the absence of liposomes, CCCP-1 remained at the bottom of the gradient. Thus, CCCP-1 directly binds membranes.

Domain structure prediction software does not indicate the presence of any canonical lipid-binding domain in CCCP-1, nor does CCCP-1 have a lipid-binding Amphipathic Lipid Packing Sensor (ALPS) motif (our unpublished observations). Thus, CCCP-1 may contain a previously uncharacterized lipid-binding domain or motif. To test whether CCCP-1 has affinity for phospholipids bearing specific head groups, we used a protein-lipid overlay assay (PIP strip) (Fig. 5D). CCCP-1 bound preferentially to phosphatidylinositides with a single phosphate group: phosphatidylinositol 3-phosphate (PI(3)P), phosphatidylinositol 4-phosphate (PI(4)P) and phosphatidylinositol 5-phosphate (PI(5)P). In addition, CCCP-1 showed some affinity for phosphatidic acid (PA) and phosphatidylserine (PS) (lipid head groups with a negative net charge), and phosphatidylethanolamine (PE) (a neutral head group) (Fig. 5D). Thus, at least in blot overlay assays, the interaction is not selective for a specific lipid and not purely electrostatic or hydrophobic. To determine whether CCCP-1 prefers binding to a specific phosphatidylinositol with a single phosphate, we performed a protein-lipid overlay assay using a membrane spotted with an increasing concentration of

phosphatidylinositols (PIP array). No obvious chemical selectivity was apparent (Fig. 5E).

Because CC3 is necessary and sufficient for CCCP-1 localization in vivo, we tested whether CCCP-1 binds membranes through CC3. In flotation assays, fragments containing CC3 (that is, CC3 or CC2+3) floated with the liposomes (Fig. 5F, lanes 5 and 6). Other CCCP-1 fragments remained mostly at the bottom; however, a small amount of CC1+2 migrated to the top of the tube (Fig. 5F, lanes 5 and 6). Because less CC3 bound to liposomes than full-length CCCP-1, the binding affinity of CC3 to membranes may be weaker. However, the CC3 protein was less stable than the full-length CCCP-1 so the decreased liposome binding of CC3 may be due to its decreased stability. We conclude that CC3 is sufficient for CCCP-1 membrane binding. Together, these results demonstrate that CC3 contains both a RAB-2 binding site and a novel membrane-association domain or motif.

CCCP-1 forms oligomers and has an elongated structure—CCCP-1 is predicted to be a coiled-coil protein with a domain structure reminiscent of the golgins, elongated proteins that act as Golgi-localized tethering factors (28–32). To test whether CCCP-1 has biophysical properties similar to golgins, we studied purified *C. elegans* CCCP-1. Though CCCP-1 has a predicted monomeric molecular mass of 89 kDa, it eluted from a Superose 6 size-exclusion column in two peaks, both with an apparent mass (M_r) larger than a 670 kDa globular protein standard (Fig. 6A). This result suggests that CCCP-1 may have an elongated non-globular shape, form oligomers, or be aggregated. Golgins are elongated and generally form oligomers (28, 29, 35). We found that CCCP-1 interacts with itself in yeast two-hybrid experiments and thus is capable of at least dimerization (data not shown).

To test for misfolding-induced aggregation, we performed circular dichroism (CD) spectroscopy. Given that CCCP-1 is predicted to be a coiled-coil protein, it should be mostly alpha-helical. We performed CD spectroscopy on the protein from each of the elution peaks. The CD scans exhibit the typical profile of a predominantly α-helical protein with minima at 208 nm and 222 nm (Fig. 6B), confirming that CCCP-1 has the expected secondary structure. Moreover, melting curves show a single sharp transition (Fig. 6B), implying that the protein is homogeneously folded. The CD scans and melting curves of protein in both elution peaks are highly similar, suggesting that the void fraction does not contain misfolded aggregates but rather CCCP-1 in a higher-order oligomeric state.

Because CCCP-1 has such a large apparent molecular mass as measured by size-exclusion chromatography, we examined its structure by negative-stain electron microscopy (EM). CCCP-1 formed elongated filaments of varying shapes and sizes (Fig. 6C), explaining why the protein runs large and suggesting that CCCP-1 may exist as polymorphic oligomers with multiple flexible forms. Similar biophysical features have been observed for other golgins (35–37).

To determine which domain of the protein is responsible for its large apparent molecular mass, we analyzed purified CCCP-1 fragments by size-exclusion chromatography. Fragments containing the CC2 middle domain (CC2, CC1+2, and CC2+3) ran as broad peaks at a very large apparent molecular weight (Fig. 6D). Furthermore, we observed that CC1 and CC3 ran as single peaks closer to but still larger than their predicted globular monomeric masses (Fig. 6D). Together, these results indicate that CCCP-1 likely forms extended oligomers and that the CC2 middle domain mediates the formation of higher-order oligomeric states, the formation of elongated structures, or both.

DISCUSSION

Here we performed a structure-function analysis of CCCP-1 to identify the important domains of the protein and assign activities to these domains. We found that the ~200 amino acid C-terminal domain (CC3) has multiple activities. First, CC3 is necessary and sufficient for localization to the trans-Golgi. Second, CC3 is necessary and sufficient for binding RAB-2. Third, CC3 mediates direct binding to a membrane bilayer. Furthermore, CC3 is required for CCCP-1 function in *C. elegans* neurons. We propose that CC3 is a novel membrane-binding domain that targets CCCP-1 to membranes and is necessary for CCCP-1 function in DCV biogenesis. Interestingly, RAB-2 is not required for the localization of CCCP-1 or its CC3 domain in vivo. Thus, the CC3 domain appears to contain the

information to target CCCP-1, even in the absence of RAB-2. Though CCCP-1 localization could theoretically be determined by its binding to membranes with specific physical and chemical properties, we found a relative lack of specificity in the interaction of CCCP-1 with lipids. Thus, CCCP-1 must also depend on additional factors for localization, or be localized through a combination of protein and lipid-binding activities.

CC3 is a novel membrane-binding domain

Our data indicate that CC3 contains a membrane-binding domain and suggest that direct membrane association is important for the function of CCCP-1. Unlike other long coiled-coil trafficking proteins, CCCP-1 does not contain a recognizable lipid-binding domain such as the GRIP domain found in golgins (GRIP = "Golgi targeting domain golgin-97, RanBP2alpha, Imh1p and p230/golgin-245") (24, 28, 29, 38). The blot overlay experiments suggest that CCCP-1 does not have chemical selectivity for a specific lipid and that it binds to both negatively-charged and neutral lipid head groups. These data raise the possibility that the interaction of CCCP-1 with membranes may depend on a combination of physical and chemical factors such as membrane curvature, electrostatics, hydrophobicity, and lipid packing. Membrane-protein interactions are often mediated by amphipathic helices such as the ALPS motif (39–41). We found that CC3 contains several potential amphipathic helices in and downstream of its predicted coiled-coil domain (Fig. S1, HeliQuest (42)), but none of them have the properties of the lipid-binding ALPS motif which contains bulky aromatic residues on the hydrophobic side of the helix and mostly noncharged residues on its polar side (34, 40, 43).

In Basic local alignment search tool (BLAST) analyses, we found a single clear CCCP-1 ortholog in most metazoans, including primitive metazoans like sponges and cnidarians (Fig. S1), though it is not apparent in other primitive metazoans including ctenophores and placozoans. Interestingly, we also found a likely CCCP-1 ortholog in two single-celled organisms closely related to metazoans: the choanoflagellate *M. brevicollis* and the snail symbiont *C. owczarzaki*. This suggests that CCCP-1 originated shortly before the origin of metazoans and was perhaps lost in some early metazoan lineages. An alignment of CCCP-1 and its orthologs shows that the C-terminal domain of CCCP-1 that includes the third coiled-coil domain and sequence downstream is the most highly conserved region of the protein (Fig. S1). The middle part of the protein shows moderate conservation and the N-terminal region is the most diverged (Fig. S1). Thus, the proposed lipid-binding and localization domain of CCCP-1 is the most highly conserved part of the protein, suggesting that it has been selected to maintain these functions and that the ancestral function of CCCP-1 may have been in membrane traffic.

Is CCCP-1 a golgin?

Several features of CCCP-1 suggest that it may be a new member of the golgin family. First, CCCP-1 has a domain structure predicted to be largely coiled-coil, and golgins belong to a family of conserved proteins that are composed of extended coiled-coil domains (28, 29). Second, like other golgins, CCCP-1 is localized to the Golgi. Third, CCCP-1 localization is mediated by its C-terminal domain, in part through direct membrane association. Similarly, golgins are often anchored by their C-termini to specific regions of the Golgi (28, 29), either through a C-terminal transmembrane anchor or a lipid-binding domain (28, 29). Fourth, both CCCP-1 and golgins form oligomers (29, 35, 36, 44). Fifth, CCCP-1 forms elongated structures like golgins (29, 35, 36, 44). Sixth, both CCCP-1 and golgins bind activated Rab proteins.

What do these similarities suggest about the molecular function of CCCP-1? Golgins often function as molecular tethers, capturing incoming vesicles at the Golgi to help mediate fusion (28, 29, 45), with different golgins tethering vesicles that emerge from different compartments (45). Perhaps CCCP-1 also functions as a molecular tether to help facilitate membrane fusion events that occur during early steps in dense-core vesicle biogenesis. Given that CCCP-1 is anchored at its C-terminus, interactions with other membrane compartments might be mediated by its N-terminal domains that may be extended away from the trans-Golgi.

What is the function of CCCP-1 in DCV biogenesis?

Why might a long coiled-coil tether be important in DCV biogenesis? There are several steps in DCV maturation that involve membrane fusion reactions that may require tethering molecules. One is the homotypic fusion of immature DCVs (4, 18, 46), a process recently shown to involve the HID-1 protein (47). Interestingly, *hid-1* mutants in *C. elegans* have defects in locomotion and DCV cargo sorting similar to *cccp-1* and *rab-2* mutants (21, 48, 49), suggesting that RAB-2 and CCCP-1 may also be important for homotypic fusion of immature DCVs. A second step of DCV maturation that may involve membrane fusion reactions is the post-Golgi "sorting by exit" of non-DCV cargos from immature DCVs (2–4, 50, 51). In *rab-2* mutants, DCV cargos are inappropriately lost to the endosomal/lysosomal system (19, 20), possibly due to overactivation of the sorting by exit pathway. Consistent with this possibility, we recently discovered that the endosomal-associated retrograde protein (EARP) complex functions in the RAB-2/CCCP-1 genetic pathway to mediate cargo sorting to DCVs. EARP is a member of the family of multisubunit tethering complexes (25, 52). Perhaps CCCP-1 interacts with EARP to mediate the Golgi tethering of endosomally-derived retrograde vesicles that contain recycled DCV cargo or sorting factors.

EXPERIMENTAL PROCEDURES

Strains—Worm strains were cultured and maintained using standard methods (53). A complete list of strains and mutations used is provided in the Strain List (Table 1).

Molecular biology and transgenes—A complete list of constructs used in this study is provided in the Plasmid List (Table 2). Using the multisite Gateway system, we cloned the full-length *cccp-1b* cDNA tagged at the C-terminal with eGFP under the expression of the *rab-3* and *cccp-1* promoters into the pCFJ150 destination vector used for Mos1-mediated single copy insertion (MosSCI) (54, 55). For the different CCCP-1 truncations, vector backbones and *cccp-1* cDNA fragments containing 20-30 bp overlapping ends were PCR amplified and combined by Gibson cloning (56, 57). All single copy integrations were made by the direct injection MosSCI method at the *ttTi5605* insertion site (54, 55). Extrachromosomal arrays were made by standard transformation methods (58). For most constructs, we isolated two or more independent lines that behaved similarly. We generated only one line overexpressing CC3::GFP under the *rab-3* promoter.

For protein expression, *C. elegans* cDNAs coding for RAB-2, CCCP-1, and CCCP-1 fragments (as shown in Fig. 1C) were inserted in pGST or pHIS parallel vectors (39) by Gibson cloning (56, 57) between the vector BamHI and XhoI restriction sites for RAB-2, and between the BamHI and EcoRI restriction sites for the other constructs.

For cloning the rat CCCP1 cDNA, rat cDNA was generated from PC12 cells using QuantiTect Reverse transcription kit (Qiagen) and an anchored Oligo(dT) primer. The CCCP1 cDNA was PCR amplified using gene specific primers and sequenced. The sequence had a few variations compared to the reported sequence and was submitted to Genbank (accession # KX954625). CCCP1 and its fragments CC1+2 (amino acids 1-743) and CC3 (amino acids 750-922) were cloned into the pEGFP-N1 vector at the EcoRI and BamH1 restriction sites using either classical restriction digest and ligation for the full length protein or Gibson cloning (34,35) with PCR amplified vector and inserts for the fragments.

C. elegans fluorescence imaging—Worms were mounted on 2% agarose pads and anesthetized with 100 mM sodium azide. To image the dorsal nerve cords, young adult animals were oriented with dorsal side up by exposure to the anesthetic for ten minutes before placing the cover slip. Images were obtained using a Nikon Eclipse 80i wide-field compound microscope with 40x or 60x oil objectives (numerical apertures of 1.30 and 1.40 respectively). Images were acquired at room temperature using an Andor Technology Neo sCMOS camera, model number DC152Q-C00-FI. The acquisition software used was NIS Elements AR 4.10.01. Raw images were then cropped with FIJI. Strains were imaged multiple times.

Cell culture—The insulinoma INS-1-derived 832/13 rat cell line was obtained from Dr. Christopher Newgard (Duke University School of Medicine) via Dr. Ian Sweet and Dr. Duk-Su Koh (University of Washington). 832/13 cells were routinely grown at 5% CO2 at 37°C in RPMI-1640, GlutaMAXTM (GIBCO), supplemented

with 10% FBS, 1 mM Sodium pyruvate, 10 mM HEPES, 50 μM 2-mercaptoethanol, and 1X Pen/Strep (GIBCO). Cells were passaged biweekly after trypsin-EDTA detachment. All studies were performed on 832/13 passages between 70 and 90.

Immunostaining of 832/13 cells— 832/13 cells were plated on a coverslip at 80-90% confluency. After 24 hours, cells were transfected with a construct expressing C-terminally EGFP-tagged rat CCCP1, CC1+2 (amino acids 1-743) or CC3 (amino acids 750-922) using Lipofectamine 2000 (Thermo Fisher) according to the manufacturer's instructions. Cells were immunostained as described (25). Primary antibodies were the rabbit polyclonal anti-TGN38 (1:350, Sigma #T9826) and mouse monoclonal anti-GFP (1:350, Santa Cruz #sc-9996). Secondary antibodies were the Rhodamine anti-rabbit secondary antibody (1:1000, Jackson Immunoresearch #111-025-144) and Alexa Fluor 488 anti-mouse secondary antibody (1:1000, Jackson Immunoresearch #115-545-146). The cells were examined by fluorescence microscopy (Nikon 80i wide-field compound microscope).

Locomotion assays—To measure locomotion, first-day adults were picked to thin lawns of OP50 bacteria (2-3 day-old plates) and body bends were counted for one minute immediately after picking. A body bend was defined as the movement of the worm from maximum to minimum amplitude of the sine wave. Worms mutant for *cccp-1*, like other mutants affecting DCV function, have a stereotypical "unmotivated" phenotype in which worms are slow when placed on food (24). In our assay conditions, in which the worm was stimulated by transfer to a new plate, expression of full length CCCP-1 fully rescued the locomotion defect of *cccp-1* mutants (Fig. 4A). However, we observed that the transgene only partially rescued the locomotion defect of a *cccp-1* mutant when worms were not stimulated. This incomplete rescue could be due to the GFP tag, differences in expression levels, or the use of cDNA in the transgenes. This result further suggests that worm locomotion is sensitive to CCCP-1 expression levels. The locomotion assays were repeated twice or more.

Protein expression in bacteria and purification—GST-RAB-2, His_6-CCCP-1, GST-CCCP-1, GST, and all His_6-CCCP-1 fragments were transformed into *E. coli* BL21 (DE3), pLys Rosetta cells (Invitrogen). His_6-CCCP-1 was grown in LB medium containing ampicillin and chloramphenicol to OD600 = 0.4-0.6. Protein expression was induced with 0.4 mM Isopropyl β-D-1-thiogalactopyranoside (IPTG) at 20°C overnight. Bacteria were harvested by a 5,000g spin at 4°C and cells were resuspended in ice-cold lysis buffer containing 50 mM Tris, pH 7.6, 200 mM NaCl, 10% glycerol, 5 mM 2-mercaptoethanol, 1-2 mM $MgCl_2$, 0.5-1% Triton-X100, up to 1 μL of benzonase nuclease (Sigma) per 10 mL of lysis buffer, and supplemented with protease inhibitor cocktail (Pierce, according to manufacturer's instructions) and 1 mM PMSF. 10-25 mM of imidazole was added in the lysis buffer to decrease nonspecific binding to the nickel resin. Cells were lysed by sonication. An additional 1 mM of PMSF was added to the lysate during sonication. Lysates were clarified by a 20,000g spin at 4°C. The supernatant was incubated with PerfectPro Ni-NTA Agarose (5 Prime) by either gravity flow using a disposable column or batch purification. The resin was washed with buffer containing 50 mM Tris, pH 7.6, 25-35 mM imidazole, 200 mM NaCl, 10% glycerol, and 5 mM 2-mercaptoethanol. The resin was eluted with the same buffer containing 250 to 400 mM imidazole.

For the His_6-CCCP-1 used for SEC, CD and EM, the eluted protein was concentrated using an Amicon-Ultra centrifugal filter, and buffer exchanged to 50 mM Tris pH 7.6, 200 mM NaCl, 5 mM 2-mercaptoethanol using a PD-10 column (GE Healthcare). Protein aliquots were flash-frozen in liquid nitrogen and stored at –80°C.

The His_6 tag of full length CCCP-1 was cleaved off using TEV protease, which was expressed and purified as described (60). An estimated 1:10 molar amount of His_6-TEV protease was added to the eluted CCCP-1 protein and incubated overnight at 4°C with gentle rotation. The protein was buffer exchanged (20 mM Tris pH 7.6, 200 mM NaCl, 2 mM 2-mercaptoethanol) by dialysis. The cleaved tag and the protease were removed by incubation with PerfectPro Ni-NTA resin for 1 hour at 4°C. Cleaved protein was concentrated, supplemented with 10% glycerol, aliquoted and flash frozen in liquid nitrogen.

His_6-CCCP-1 fragments were grown in TB medium containing ampicillin and chloramphenicol to OD600 = 0.8-1 and protein expression was induced with 1 mM IPTG. The protein was handled like His_6-CCCP-1 full length except that the lysis buffer lacked benzonase and $MgCl_2$. The eluted protein was dialyzed with 20 mM Tris pH 7.6, 200 mM NaCl, 2 mM 2-mercaptoethanol, concentrated, supplemented with 10% glycerol, aliquoted and flash frozen in liquid nitrogen.

For the GST-CCCP-1 and GST used for the protein-lipid overlay assays, cells were grown in TB medium containing ampicillin and chloramphenicol to OD600 = 0.5-0.8 and protein expression was induced with 0.5 mM IPTG. After induction, bacteria were then incubated at 20°C overnight. Harvested cells were resuspended in the same ice-cold lysis buffer described above for His_6-tagged proteins except lacking imidazole, benzonase and $MgCl_2$ and lysed by sonication. The clarified lysate was incubated with GST-Sepharose resin (GE Healthcare). The resin was then washed with 50 mM Tris, pH 7.6, 200 mM NaCl, 10% glycerol, 5 mM 2-mercaptoethanol and eluted with the same buffer containing 20 mM reduced glutathione. The eluted protein was dialyzed (20 mM Tris pH 7.6, 200 mM NaCl, 2 mM 2-mercaptoethanol, supplemented with 10% glycerol), aliquoted and flash frozen in liquid nitrogen.

GST-RAB-2 and GST used for the GST-RAB-2 pull downs were grown in LB medium containing ampicillin and chloramphenicol to OD600 = 0.4-0.6. Protein expression was induced with 1 mM IPTG at 18°C overnight. Bacteria were harvested and resuspended in ice-cold lysis buffer containing 50 mM Tris, pH 7.6, 200 mM NaCl, 10% glycerol, 5 mM 2-mercaptoethanol, 2 mM $MgCl_2$, 0.2% Triton-X100, up to 1 µL of benzonase nuclease (Sigma) per 10 mL of lysis buffer and supplemented with protease inhibitor cocktail (Pierce, according to manufacturer's instructions) and 1 mM PMSF. Cells were lysed as above and stored as a clarified lysate at -80°C. The concentration of GST or GST-RAB-2 in the lysate was estimated by a small-scale affinity purification.

Protein expression and purification conditions typically yielded more than 1 mg of protein per liter of culture media. The protein concentration was measured with Bradford reagent and purity was assessed with Coomassie-stained SDS-PAGE. GST-tagged proteins were estimated to be over 95% pure. CCCP-1 fragments containing CC3, especially CC3 alone, yielded less protein and the measured concentration of protein was adjusted by comparing the band intensity with purer His_6-tagged fragments on a Western blot. All proteins migrated on SDS-PAGE to their expected molecular weight, except for GST-RAB-2 (predicted 50 kDa) that migrated between the 37 kDa marker and the 50 kDa marker, and His_6-CC1 fragment (predicated 19 kDa) that migrated above the 20 kDa marker.

Western blotting—Protein samples were solubilized in SDS loading dye and resolved on 8%, 10% or 12% SDS-PAGE gels. Proteins were then transferred to PVDF or nitrocellulose membranes using a semi-dry transfer apparatus (Biorad) system. The membranes were blocked with 3% dry milk in TBST (10 mM Tris pH 7.4, 150 mM NaCl, 0.05% Tween-20) for 1 hour at room temperature or overnight at 4°C. Primary and secondary antibodies were diluted in TBST + 3% dry milk and incubated 1 hour at room temperature or overnight at 4°C. The following primary antibodies were used: mouse monoclonal anti-His_6 (1:1000, Thermo Scientific HIS.H8 #MA1-21315), mouse monoclonal anti-GFP (1:1000, Roche #11814460001), mouse monoclonal anti-beta-tubulin antibody (1:1000, Thermo Scientific #MA5-16308) and rabbit polyclonal anti-Rab2 (1:200, Santa Cruz Biotechnology (FL-212) sc-28567, produced from a human RAB2A antigen). The secondary antibodies were: Alexa Fluor 680-conjugated affinity pure goat anti-mouse antibody (1:20,000, Jackson Immunoresearch #115-625-166) and Alexa Fluor 680-conjugated affinity pure goat anti-rabbit antibody (1:20,000 Jackson Immunoresearch #111-625-144). A Li-COR processor was used to develop images.

GST-RAB-2 pulldowns—To decrease nonspecific binding, we used LoBind microcentrifuge tubes (Eppendorf). 25 µL of glutathione sepharose resin (GE Healthcare) was blocked for 1 hour at room temperature or overnight at 4°C with 5% bovine serum albumin (BSA) in reaction buffer (50 mM Tris pH 7.6, 150 mM NaCl, 10% glycerol, 5 mM 2-mercaptoethanol, 5 mM $MgCl_2$ and 1% Triton-X100). The resin was washed with reaction buffer

and incubated with clarified bacterial lysates containing about 50 μg of GST-RAB-2 or 25 μg of GST for 1 hour at 4°C with gentle agitation. Beads were washed with nucleotide loading buffer (50 mM Tris pH 7.6, 150 mM NaCl, 10% glycerol, 5 mM 2-mercaptoethanol, 5 mM EDTA and 1% Triton-X100) and incubated with either 60X molar ratio of GTPγS or 300X of GDP on a rotator at room temperature for 2 hours. 20 mM $MgCl_2$ was added to the reaction and incubated for another 15 minutes at room temperature. Nucleotides were washed off with reaction buffer and the beads were incubated with CCCP-1 or its fragments (at 1 to 2 molar ratio with GST-RAB-2) for 2 hours at 4°C on a rotator. Beads were washed three times with low volumes of reaction buffer (3 x 200 μL) and the resin was eluted with 20 mM reduced glutathione in reaction buffer. Half of the eluent was loaded on SDS-PAGE gels and analyzed by Western blotting against the His_6-tag. The pulldown was repeated four times with the full-length protein and twice with the fragments with identical results.

Cell fractionation—We used a similar method to the one described (52). Specifically, 832/13 cells were grown on a 15 cm dish to 90% confluence and transfected with CCCP1::eGFP using Lipofectamine 2000 (Thermo Fisher) according to the manufacturer's instructions. After 24 h, cells were washed twice with ice cold PBS and detached using a cell scraper. Cells were then transferred to a microcentrifuge tube and pelleted for 5 min at 300g in a tabletop centrifuge at 4°C. Cells were resuspended in 500 μL sucrose buffer (20 mM HEPES, pH 7.4, 250 mM sucrose supplemented with protease inhibitors (Pierce) and 1 mM PMSF) and were homogenized on ice by a Dounce homogenizer (20 strokes). The cell lysate was then centrifuged at 1,000g for 5 minutes at 4°C to remove unbroken cells and nuclear debris. The post-nuclear supernatant was further clarified by centrifugation at 13,000g for 10 min at 4°C. The supernatant was divided into four samples, one of which was supplemented with SDS loading buffer (supernatant, S13). Membranes in the other three samples were pelleted using a Beckman TLA100 rotor (45 minutes, 90,000g, 4°C). The supernatant from one of the samples was supplemented with SDS page loading buffer (supernatant, S90) and its pellet was resuspended in an equal volume of sucrose buffer and supplemented with SDS loading buffer (pellet, P90). The pellets of the two last samples were resuspended in either high-salt buffer (50 mM Tris, pH 7.4, 1 M NaCl, 1 mM EDTA supplemented with 10% glycerol and protease inhibitors) or detergent buffer (50 mM Tris, pH 7.4, 150 mM NaCl, 1% Triton X-100, 1 mM EDTA supplemented with 10% glycerol and protease inhibitors). After incubation for 1 hour on ice the samples were centrifuged at 90,000g for 45 min at 4°C. The collected membrane fractions, either salt-extracted (S90, 1 M NaCl) or detergent-extracted (S90, 1% Triton X-100), were then supplemented with SDS loading buffer. Their pellets were resuspended in equal volumes of high salt or detergent buffer and then supplemented with SDS loading buffer (P90, 1 M NaCl and P90, 1% Triton X-100). Samples were analyzed by Western blot. The experiment was repeated twice.

Golgi-mix liposome preparation—The following lipids were used: 1-palmitoyl-2-oleoyl-sn-glycero-3-phosphocholine (POPC), 1,2-dipalmitoyl-sn-glycero-3-phosphoethanolamine (DPPE), and 1,2-di-oleoyl-sn-glycero-3-phospho-l-serine (DOPS) were purchased from NOF America Corporation. Cholesterol, L-α-phosphatidylinositol from soy (PI) and 1,2-dioleoyl-sn-glycero-3-phosphoethanolamine-N-(lissamine rhodamine B sulfonyl) (Rh-PE) were purchased from Avanti Polar Lipids. The composition of Golgi-mix liposomes was as described (34) with the following fractions given as molar percent: POPC (49%), DPPE (19%), DOPS (5%), Soy-PI (10 %), cholesterol (16%) and Rhodamine-PE (1%). The lipids dissolved in chloroform were mixed together and chloroform was dried under compressed nitrogen for 3 hours to overnight and then lyophilized in a Labconco Free Zone 2.5 lyophilizer for 1 hour to remove residual chloroform. The dried lipid mixture was resuspended in 50 mM Tris pH 7.6 and 50 mM NaCl. To generate the liposomes, the mixture was sonicated for 5 minutes in a 50°C water bath. Liposomes were stored at room temperature and used within 2-3 days.

Flotation experiments—Proteins (1 μM) and Golgi-mix liposomes (1 mM) were incubated in 50 mM Tris pH 7.6, 50 mM NaCl buffer at room temperature for 30 minutes. The suspension was adjusted to 40% sucrose by adding 75% w/v sucrose solution in the same buffer for a total

volume of 200 µL and transferred to a polycarbonate ultracentrifuge tube (Beckman Coulter, 343778). Three layers were overlaid on top of the high sucrose suspension: 500 µL of 30% sucrose, 300 µL of 10% sucrose and 200 µL of 0% sucrose in 50 mM Tris pH 7.6, 50 mM NaCl. The sample was centrifuged at 200,000g in a Beckman Coulter swinging bucket rotor (TLS 55) for 2 hours at 25°C. Most of the fluorescently labeled liposomes migrated to the top of the tube in three layers close to the 0%-10% sucrose interface. Six fractions of 200 µL each were collected from the top. The second fraction contained most of the pink color coming from rhodamine, with some in the third fraction as well. Experiments with full-length untagged CCCP-1 were analyzed by SDS-PAGE and Coomassie blue staining. Experiments with the His_6-tagged CCCP-1 fragments were analyzed by Western blot using an antibody to the His_6 epitope tag. Experiments with the full-length CCCP-1 protein were performed three times with two independent liposome preparations. Experiments with CC3 were performed three times, CC1+2 twice, CC1 twice, CC2 and CC2+3 once. The key experiments with CC3 and CC1+2 were performed side by side twice with independent liposome preparations and both showed CC3 as a much stronger liposome binder.

PIP Strips and PIP arrays—The PIP strips and PIP arrays were purchased from Echelon and used as recommended by the manufacturer. The membranes were blocked for 1 hour at room temperature with PBST (0.1% v/v Tween-20) + 3% fatty acid-free BSA (Sigma). The membranes were incubated for 1 hour at room temperature with GST or GST-CCCP-1. For the PIP strip, equimolar amounts of GST and GST-CCCP-1 were used (around 100 nM in PBST + 3% fatty acid-free BSA). For the PIP array, 70 nM of GST-CCCP-1 and 150 nM of GST were used. The membranes were washed with PBST and incubated with the anti-GST antibody Horseradish Peroxidase (HRP) conjugate (K-SEC2 from Echelon) in PBST + 3% fatty acid-free BSA. Lipid binding was detected by adding 3,3',5,5'-tetramethylbenzidine (TMB) precipitating solution (K-TMB from Echelon). The positive control PI(4,5)P2 Grip (PLC-δ1-PH) was obtained from Echelon (Catalog #G-4501) and used as recommended by the manufacturer. The membranes were imaged with a conventional digital camera. The experiment was performed once each.

Size-exclusion chromatography (SEC)—Aliquots of His_6-CCCP-1 expressed and purified as described above were loaded on a Superose 6 column (GE Healthcare) at 4°C. His_6-CCCP-1 was eluted with 50 mM Tris pH 7.6, 200 mM NaCl and 5 mM 2-mercaptoethanol. Given that CCCP-1 does not contain any tryptophan residues, its extinction coefficient is very low. Since the size-exclusion chromatogram was very sensitive to more optically absorbent contaminants, we collected 1 mL fractions and analyzed them by Coomassie-stained SDS-PAGE gels. His_6-CCCP-1 fractions (fractions 8-9 and 11-12, Fig. 6A, colored bars) were concentrated around 10-fold using an Amicon Ultra centrifugal unit and flash frozen in liquid nitrogen. Recombinant His_6-CCCP-1 fragments were loaded on a Superose 6 (or Superdex 200) column and eluted with 50 mM Tris pH 7.6 and 200 mM NaCl. Fractions were analyzed by Western blot to the His_6 tag. For the full-length CCCP-1 protein, the SEC experiment was repeated at least three times on independent protein preparations, and untagged CCCP-1 had an identical elution profile to the tagged protein. The CCCP-1 fragments were analyzed by SEC twice or more from a single protein prep, except for CC3 that was analyzed from multiple independent preps.

Circular dichroism spectroscopy—Samples were analyzed using a Jasco J-1500 circular dichroism (CD) spectrometer. Protein in 50 mM Tris pH 7.6, 200 mM NaCl and 5 mM 2-mercaptoethanol was used to collect the CD data. The signal was blanked with buffer only. For the CD scan, the samples were kept at 4°C and the ellipticity (in mdeg) was measured at wavelengths between 195 nm and 260 nm. For the melting curve, the ellipticity (mdeg) was measured at 222 nm as the temperature was increasing from 4°C to 100°C. The experiment was performed twice with two independent protein preparations.

Negative-stain electron microscopy—Aliquots of fractions 11-12 from size-exclusion chromatography (see above) were diluted to 0.01 mg/mL in 50 mM Tris pH 7.6, 200 mM NaCl and 5 mM 2-mercaptoethanol. Samples were prepared by negative stain, using a 0.7% uranyl formate solution, and spotted onto a 400 mesh copper-

coated grid. Electron micrographs were acquired on a Tecnai T12 microscope (FEI co.), operating at 120 kV, at 52,000X magnification, with images taken by a Gatan US4000 CCD camera. Similar results were observed using protein from an independent protein preparation and imaged using a Morgagni M268 electron microscope.

Statistics—Data were tested for normality by a Shapiro-Wilk test. We used the Kruskal-Wallis test followed by Dunn's test to investigate whether there was statistical significance between groups.

Acknowledgments

We thank Kumud Raj Poudel and Jihong Bai for sharing purified phospholipids and for help with generating liposomes; Amanda Clouser for help with CD spectroscopy; Duk-Su Koh for the 832/13 and PC12 cell lines; Suzanne Hoppins for sharing equipment and experimental guidance; Maximillian Greenwald for assistance with *C. elegans* locomotion assays; Andrew Borst for help with electron microscopy; and Jihong Bai for comments on the manuscript. JC was supported in part by an NIH Institutional Training Grant for Neurobiology (T32 GM007108). This work was supported by NIH grant R01 GM077349 to AJM and by NIH grant R00 MH082109 and an Ellison Medical Foundation New Scholar Award to MA.

Conflict of Interests

The authors declare that they have no conflicts of interest with the contents of this article.

Author contributions

JC conducted most of the experiments and analyzed most of the results. IT maintained the mammalian cell culture, prepared the cells for the biochemical cell fractionation, and performed mammalian cell immunostaining and imaging experiments. AD operated the electron microscope and generated the electron micrographs. JC wrote the paper with the help of IT, MA and AJM. AJM and MA supervised the project.

REFERENCES

1. Tooze, S. A., Martens, G. J., and Huttner, W. B. (2001) Secretory granule biogenesis: rafting to the SNARE. *Trends Cell Biol.* **11**, 116–122
2. Morvan, J., and Tooze, S. A. (2008) Discovery and progress in our understanding of the regulated secretory pathway in neuroendocrine cells. *Histochem. Cell Biol.* **129**, 243–252
3. Borgonovo, B., Ouwendijk, J., and Solimena, M. (2006) Biogenesis of secretory granules. *Curr. Opin. Cell Biol.* **18**, 365–370
4. Gondré-Lewis, M. C., Park, J. J., and Loh, Y. P. (2012) Cellular mechanisms for the biogenesis and transport of synaptic and dense-core vesicles. *Int. Rev. Cell Mol. Biol.* **299**, 27–115
5. Bonnemaison, M., Bäck, N., Lin, Y., Bonifacino, J. S., Mains, R., and Eipper, B. (2014) AP-1A controls secretory granule biogenesis and trafficking of membrane secretory granule proteins. *Traffic*. **15**, 1099–1121
6. Asensio, C. S., Sirkis, D. W., and Edwards, R. H. (2010) RNAi screen identifies a role for adaptor protein AP-3 in sorting to the regulated secretory pathway. *J. Cell Biol.* **191**, 1173–1187
7. Asensio, C. S., Sirkis, D. W., Maas Jr., J. W., Egami, K., To, T.-L., Brodsky, F. M., Shu, X., Cheng, Y., and Edwards, R. H. (2013) Self-assembly of VPS41 promotes sorting required for biogenesis of the regulated secretory pathway. *Dev. Cell*. **27**, 425–437
8. Walter, A. M., Kurps, J., Wit, H. de, Schöning, S., Toft-Bertelsen, T. L., Lauks, J., Ziomkiewicz, I., Weiss, A. N., Schulz, A., Mollard, G. F. von, Verhage, M., and Sørensen, J. B. (2014) The SNARE protein vti1a functions in dense-core vesicle biogenesis. *EMBO J.* **33**, 1681–1697
9. Buffa, L., Fuchs, E., Pietropaolo, M., Barr, F., and Solimena, M. (2008) ICA69 is a novel Rab2 effector regulating ER–Golgi trafficking in insulinoma cells. *Eur. J. Cell Biol.* **87**, 197–209
10. Cao, M., Mao, Z., Kam, C., Xiao, N., Cao, X., Shen, C., Cheng, K. K. Y., Xu, A., Lee, K.-M., Jiang, L., and Xia, J. (2013) PICK1 and ICA69 control insulin granule trafficking and their deficiencies lead to impaired glucose tolerance. *PLoS Biol*. **11**, e1001541
11. Holst, B., Madsen, K. L., Jansen, A. M., Jin, C., Rickhag, M., Lund, V. K., Jensen, M., Bhatia, V., Sørensen, G., Madsen, A. N., Xue, Z., Møller, S. K., Woldbye, D., Qvortrup, K., Huganir, R., Stamou, D., Kjærulff, O., and Gether, U. (2013) PICK1 deficiency impairs secretory vesicle

biogenesis and leads to growth retardation and decreased glucose tolerance. *PLoS Biol*. **11**, e1001542

12. Pinheiro, P. S., Jansen, A. M., Wit, H. de, Tawfik, B., Madsen, K. L., Verhage, M., Gether, U., and Sørensen, J. B. (2014) The BAR domain protein PICK1 controls vesicle number and size in adrenal chromaffin cells. *J. Neurosci.* **34**, 10688–10700
13. Kebede, M. A., Oler, A. T., Gregg, T., Balloon, A. J., Johnson, A., Mitok, K., Rabaglia, M., Schueler, K., Stapleton, D., Thorstenson, C., Wrighton, L., Floyd, B. J., Richards, O., Raines, S., Eliceiri, K., Seidah, N. G., Rhodes, C., Keller, M. P., Coon, J. L., Audhya, A., and Attie, A. D. (2014) SORCS1 is necessary for normal insulin secretory granule biogenesis in metabolically stressed β cells. *J. Clin. Invest.* **124**, 4240–4256
14. Hao, Z., Wei, L., Feng, Y., Chen, X., Du, W., Ma, J., Zhou, Z., Chen, L., and Li, W. (2015) Impaired maturation of large dense-core vesicles in muted-deficient adrenal chromaffin cells. *J. Cell Sci.* **128**, 1365–1374
15. Torres, I. L., Rosa-Ferreira, C., and Munro, S. (2014) The Arf family G protein Arl1 is required for secretory granule biogenesis in Drosophila. *J. Cell Sci.* **127**, 2151–2160
16. Burgess, J., Jauregui, M., Tan, J., Rollins, J., Lallet, S., Leventis, P. A., Boulianne, G. L., Chang, H. C., Borgne, R. L., Krämer, H., and Brill, J. A. (2011) AP-1 and clathrin are essential for secretory granule biogenesis in Drosophila. *Mol. Biol. Cell*. **22**, 2094–2105
17. Ahras, M., Otto, G. P., and Tooze, S. A. (2006) Synaptotagmin IV is necessary for the maturation of secretory granules in PC12 cells. *J. Cell Biol.* **173**, 241–251
18. Wendler, F., Page, L., Urbé, S., and Tooze, S. A. (2001) Homotypic fusion of immature secretory granules during maturation requires syntaxin 6. *Mol. Biol. Cell*. **12**, 1699–1709
19. Edwards, S. L., Charlie, N. K., Richmond, J. E., Hegermann, J., Eimer, S., and Miller, K. G. (2009) Impaired dense core vesicle maturation in Caenorhabditis elegans mutants lacking Rab2. *J. Cell Biol.* **186**, 881–895
20. Sumakovic, M., Hegermann, J., Luo, L., Husson, S. J., Schwarze, K., Olendrowitz, C., Schoofs, L., Richmond, J., and Eimer, S. (2009) UNC-108/RAB-2 and its effector RIC-19 are involved in dense core vesicle maturation in Caenorhabditis elegans. *J. Cell Biol.* **186**, 897–914
21. Mesa, R., Luo, S., Hoover, C. M., Miller, K., Minniti, A., Inestrosa, N., and Nonet, M. L. (2011) HID-1, a new component of the peptidergic signaling pathway. *Genetics*. **187**, 467–483
22. Hannemann, M., Sasidharan, N., Hegermann, J., Kutscher, L. M., Koenig, S., and Eimer, S. (2012) TBC-8, a putative RAB-2 GAP, regulates dense core vesicle maturation in Caenorhabditis elegans. *PLoS Genet*. **8**, e1002722
23. Sasidharan, N., Sumakovic, M., Hannemann, M., Hegermann, J., Liewald, J. F., Olendrowitz, C., Koenig, S., Grant, B. D., Rizzoli, S. O., Gottschalk, A., and Eimer, S. (2012) RAB-5 and RAB-10 cooperate to regulate neuropeptide release in Caenorhabditis elegans. *Proc. Natl. Acad. Sci.* **109**, 18944–18949
24. Ailion, M., Hannemann, M., Dalton, S., Pappas, A., Watanabe, S., Hegermann, J., Liu, Q., Han, H.-F., Gu, M., Goulding, M. Q., Sasidharan, N., Schuske, K., Hullett, P., Eimer, S., and Jorgensen, E. M. (2014) Two Rab2 interactors regulate dense-core vesicle maturation. *Neuron*. **82**, 167–180
25. Topalidou, I., Cattin-Ortolá, J., Pappas, A. L., Cooper, K., Merrihew, G. E., MacCoss, M. J., and Ailion, M. (2016) The EARP complex and its interactor EIPR-1 are required for cargo sorting to dense-core vesicles. *PLoS Genet.* **12**, e1006074.
26. Stenmark, H. (2009) Rab GTPases as coordinators of vesicle traffic. *Nat. Rev. Mol. Cell Biol.* **10**, 513–525
27. Gillingham, A. K., Sinka, R., Torres, I. L., Lilley, K. S., and Munro, S. (2014) Toward a comprehensive map of the effectors of Rab GTPases. *Dev. Cell*. **31**, 358–373
28. Gillingham, A. K., and Munro, S. (2003) Long coiled-coil proteins and membrane traffic. *Biochim. Biophys. Acta*. **1641**, 71–85
29. Gillingham, A. K., and Munro, S. (2016) Finding the Golgi: golgin coiled-coil proteins show the way. *Trends Cell Biol.* 10.1016/j.tcb.2016.02.005

30. Witkos, T. M., and Lowe, M. (2016) The golgin family of coiled-coil tethering proteins. *Front. Cell Dev. Biol.* 10.3389/fcell.2015.00086
31. Yu, I.-M., and Hughson, F. M. (2010) Tethering factors as organizers of intracellular vesicular traffic. *Annu. Rev. Cell Dev. Biol.* **26**, 137–156
32. Sztul, E., and Lupashin, V. (2009) Role of vesicle tethering factors in the ER-Golgi membrane traffic. *FEBS Lett.* **583**, 3770–3783
33. Hohmeier, H. E., Mulder, H., Chen, G., Henkel-Rieger, R., Prentki, M., and Newgard, C. B. (2000) Isolation of INS-1-derived cell lines with robust ATP-sensitive K+ channel-dependent and -independent glucose-stimulated insulin secretion. *Diabetes*. **49**, 424–430
34. Bigay, J., Casella, J.-F., Drin, G., Mesmin, B., and Antonny, B. (2005) ArfGAP1 responds to membrane curvature through the folding of a lipid packing sensor motif. *EMBO J.* **24**, 2244–2253
35. Sapperstein, S. K., Walter, D. M., Grosvenor, A. R., Heuser, J. E., and Waters, M. G. (1995) p115 is a general vesicular transport factor related to the yeast endoplasmic reticulum to Golgi transport factor Uso1p. *Proc. Natl. Acad. Sci. U. S. A.* **92**, 522–526
36. Ishida, R., Yamamoto, A., Nakayama, K., Sohda, M., Misumi, Y., Yasunaga, T., and Nakamura, N. (2015) GM130 is a parallel tetramer with a flexible rod-like structure and N–terminally open (Y-shaped) and closed (I-shaped) conformations. *FEBS J.* **282**, 2232–2244
37. Cheung, P. P., Limouse, C., Mabuchi, H., and Pfeffer, S. R. (2016) Protein flexibility is required for vesicle tethering at the Golgi. *eLife*. **4**, e12790
38. Munro, S., and Nichols, B. J. (1999) The GRIP domain – a novel Golgi-targeting domain found in several coiled-coil proteins. *Curr. Biol.* **9**, 377–380
39. Antonny, B., Beraud-Dufour, S., Chardin, P., and Chabre, M. (1997) N-terminal hydrophobic residues of the G-protein ADP-ribosylation factor-1 insert into membrane phospholipids upon GDP to GTP exchange. *Biochemistry*. **36**, 4675–4684
40. Drin, G., and Antonny, B. (2010) Amphipathic helices and membrane curvature. *FEBS Lett.* **584**, 1840–1847
41. Miller, M. B., Vishwanatha, K. S., Mains, R. E., and Eipper, B. A. (2015) An N-terminal amphipathic helix binds phosphoinositides and enhances kalirin Sec14 domain-mediated membrane interactions. *J. Biol. Chem.* **290**, 13541–13555
42. Gautier, R., Douguet, D., Antonny, B., and Drin, G. (2008) HELIQUEST: a web server to screen sequences with specific α-helical properties. *Bioinformatics*. **24**, 2101–2102
43. Drin, G., Casella, J.-F., Gautier, R., Boehmer, T., Schwartz, T. U., and Antonny, B. (2007) A general amphipathic α-helical motif for sensing membrane curvature. *Nat. Struct. Mol. Biol.* **14**, 138–146
44. Brown, F. C., Schindelhaim, C. H., and Pfeffer, S. R. (2011) GCC185 plays independent roles in Golgi structure maintenance and AP-1–mediated vesicle tethering. *J. Cell Biol.* **194**, 779–787
45. Wong, M., and Munro, S. (2014) The specificity of vesicle traffic to the Golgi is encoded in the golgin coiled-coil proteins. *Science*. **346**, 1256898
46. Urbé, S., Page, L. J., and Tooze, S. A. (1998) Homotypic fusion of immature secretory granules during maturation in a cell-free assay. *J Cell Biol*. **143**, 1831–1844
47. Du, W., Zhou, M., Zhao, W., Cheng, D., Wang, L., Lu, J., Song, E., Feng, W., Xue, Y., Xu, P., and Xu, T. (2016) HID-1 is required for homotypic fusion of immature secretory granules during maturation. *eLife*. **5**, e18134
48. Ailion, M., and Thomas, J. H. (2003) Isolation and characterization of high-temperature-induced dauer formation mutants in Caenorhabditis elegans. *Genetics*. **165**, 127–144
49. Yu, Y., Wang, L., Jiu, Y., Zhan, Y., Liu, L., Xia, Z., Song, E., Xu, P., and Xu, T. (2011) HID-1 is a novel player in the regulation of neuropeptide sorting. *Biochem. J.* **434**, 383–390
50. Arvan, P., and Halban, P. A. (2004) Sorting ourselves out: seeking consensus on trafficking in the beta-cell. *Traffic*. **5**, 53–61

51. Klumperman, J., Kuliawat, R., Griffith, J. M., Geuze, H. J., and Arvan, P. (1998) Mannose 6-phosphate receptors are sorted from immature secretory granules via adaptor protein AP-1, clathrin, and syntaxin 6-positive vesicles. *J. Cell Biol.* **141**, 359–371
52. Schindler, C., Chen, Y., Pu, J., Guo, X., and Bonifacino, J. S. (2015) EARP is a multisubunit tethering complex involved in endocytic recycling. *Nat. Cell Biol.* 10.1038/ncb3129
53. Brenner, S. (1974) The genetics of Caenohabditis elegans. *Genetics*. **77**, 71–94
54. Frøkjær-Jensen, C., Davis, M. W., Hopkins, C. E., Newman, B., Thummel, J. M., Olesen, S.-P., Grunnet, M., and Jorgensen, E. M. (2008) Single copy insertion of transgenes in C. elegans. *Nat. Genet.* **40**, 1375–1383
55. Frøkjær-Jensen, C., Davis, M. W., Ailion, M., and Jorgensen, E. M. (2012) Improved Mos1-mediated transgenesis in C. elegans. *Nat. Methods*. **9**, 117–118
56. Gibson, D. G., Young, L., Chuang, R.-Y., Venter, J. C., Hutchison, C. A., and Smith, H. O. (2009) Enzymatic assembly of DNA molecules up to several hundred kilobases. *Nat. Methods*. **6**, 343–345
57. Gibson, D. (2009) One-step enzymatic assembly of DNA molecules up to several hundred kilobases in size. *Protoc. Exch.* 10.1038/nprot.2009.77
58. Mello, C. C., Kramer, J. M., Stinchcomb, D., and Ambros, V. (1991) Efficient gene transfer in C.elegans: extrachromosomal maintenance and integration of transforming sequences. *EMBO J.* **10**, 3959–3970
59. Sheffield, P., Garrard, S., and Derewenda, Z. (1999) Overcoming expression and purification problems of RhoGDI using a family of "parallel" expression vectors. *Protein Expr. Purif.* **15**, 34–39
60. Tropea, J. E., Cherry, S., and Waugh, D. S. (2009) Expression and purification of soluble His6-tagged TEV protease. In *High Throughput Protein Expression and Purification: Methods and Protocols* (Doyle, S. A. ed), pp. 297–307, Humana Press, Totowa, NJ

FOOTNOTES

The abbreviations used are: DCV, dense-core vesicle; CC, coiled-coil; CC3, C terminal domain of CCCP-1 (amino acids 551-743 for the *C. elegans* protein, amino acids 750-922 for the rat ortholog); CC1, N terminal domain of CCCP-1 (amino acids 1-140); CC2, middle domain of CCCP-1 (amino acids 133-743); CC1+2, fragment of CCCP-1 containing CC1 and CC2 (amino acids 1-557 for *C. elegans* CCCP-1, amino acids 1-743 for the rat protein); CC2+3, fragment of CCCP-1 containing CC2 and CC3 (amino acids 133-743); SEC, size-exclusion chromatography; CD, circular dichroism; EM, electron microscopy; GTPγS, 5'-O-[gamma-thio]triphosphate; Rh-PE, 1,2-dioleoyl-sn-glycero-3-phosphoethanolamine-N-(lissamine rhodamine B sulfonyl); POPC, 1-palmitoyl-2-oleoyl-sn-glycero-3-phosphocholine; GRIP, Golgi targeting domain golgin-97, RanBP2alpha, Imh1p and p230/golgin-245; ALPS, Amphipathic lipid packing sensor motif; PI(3)P, phosphatidylinositol 3-phosphate; PI(4)P, phosphatidylinositol 4-phosphate; PI(5)P, phosphatidylinositol 5-phosphate; PA, phosphatidic acid; PS, phosphatidylserine; PE, phosphatidylethanolamine; DPPE, 1,2-dipalmitoyl-sn-glycero-3-phosphoethanolamine; DOPS, 1,2-di-oleoyl-sn-glycero-3-phospho-l-serin; Soy PI, L-α-phosphatidylinositol; LPA, lysophosphatidic acid; LPC, lysophosphocholine; PI, phosphatidylinositol; PC, phosphatidylcholine; S1P, sphingosine 1-phosphate; PI(3,4)P2, phosphatidylinositol (3,4) bisphosphate; PI(3,5)P2, phosphatidylinositol (3,5) bisphosphate; PI(4,5)P2, phosphatidylinositol (4,5) bisphosphate; PI(3,4,5)P3, phosphatidylinositol (3,4,5) trisphosphate; BLAST, Basic local alignment search tool; IPTG, Isopropyl β-D-1-thiogalactopyranoside; TBST, tris-buffered saline supplemented with 0.05% Tween-20; PBST, phosphate-buffered saline supplemented with 0.1% Tween-20.

Table 1— Strain list

EG334	*cccp-1(ox334) III*
EG5627	*rab-2(nu415) I*
XZ1804	*yakEx101*[*Prab-3::cccp-1* cDNA::eGFP, *Pmyo-3::mcherry*]

XZ1808	*yakEx99*[*Prab-3::CC2+3* cDNA::eGFP, *Pmyo-3::mcherry*]
XZ1803	*yakEx100*[*Prab-3::CC3* cDNA::eGFP, *Pmyo-3::mcherry*]
XZ1801	*yakEx98*[*Prab-3::CC1+2* cDNA::eGFP, *Pmyo-3::mcherry*]
XZ1813	*rab-2(nu415) I; yakEx101*[*Prab-3::cccp-1* cDNA::eGFP, *Pmyo-3::mcherry*]
XZ1812	*rab-2(nu415) I; yakEx99*[*Prab-3::CC2+3* cDNA::eGFP, *Pmyo-3::mcherry*]
XZ1810	*rab-2(nu415) I; yakEx100*[*Prab-3::CC3* cDNA::eGFP , *Pmyo-3::mcherry*]
XZ1809	*rab-2(nu415) I; yakEx98*[*Prab-3::CC1+2* cDNA::eGFP, *Pmyo-3::mcherry*]
XZ1877	*oxIs602*[*cb-unc-119(+), Pcccp-1::cccp-1* cDNA::eGFP] II ; *cccp-1(ox334)* III
XZ1807	*yakSi21*[*Pcccp-1::CC1+2* cDNA::eGFP, *cb-unc-119(+)]* II ; *cccp-1(ox334)* III
XZ1893	*yakSi23*[*Pcccp-1::CC2+3* cDNA::eGFP, *cb-unc-119(+)]* II ; *cccp-1(ox334)* III
XZ1897	*yakSi25*[*Pcccp-1::CC3* cDNA::eGFP, *cb-unc-119(+)]* II ; *cccp-1(ox334)* III

Table 2—Plasmid list

<u>*C. elegans* vectors</u>
pMA59 *Prab-3::cccp-1* cDNA::eGFP in pCFJ150
pJC200 *Prab-3::CC2+3* cDNA::eGFP in pCFJ150
pJC201 *Prab-3::CC1+2* cDNA::eGFP in pCFJ150
pJC198 *Prab-3::CC3* cDNA::eGFP in pCFJ150
pMA58 *Pcccp-1::cccp-1* cDNA::eGFP in pCFJ150
pJC187 *Pcccp-1::CC2+3* cDNA::eGFP in pCFJ150
pJC188 *Pcccp-1::CC1+2* cDNA::eGFP in pCFJ150
pJC193 *Pcccp-1::CC3* cDNA::eGFP in pCFJ150

<u>Bacterial expression vectors</u>
pGST parallel
pHIS parallel
pJC121 His_6-CCCP-1 in pHIS parallel
pJC158 His_6-CC1 in pHIS parallel
pJC159 His_6-CC1+2 in pHIS parallel
pJC160 His_6-CC3 in pHIS parallel
pJC161 His_6-CC2+3 in pHIS parallel
pJC190 His_6-CC2 in pHIS parallel
pJC164 GST-CCCP-1 in pGST parallel
pJC116 GST-RAB-2
pRK793 TEV protease S219V

<u>Mammalian cell expression vectors</u>
pET50 CCCP1::GFP (rat cDNA) in pEGFP-N1
pET159 CC1+2::GFP (rat cDNA) in pEGFP-N1
pJC218 CC3::GFP (rat cDNA) in pEGFP-N1

Figure 1

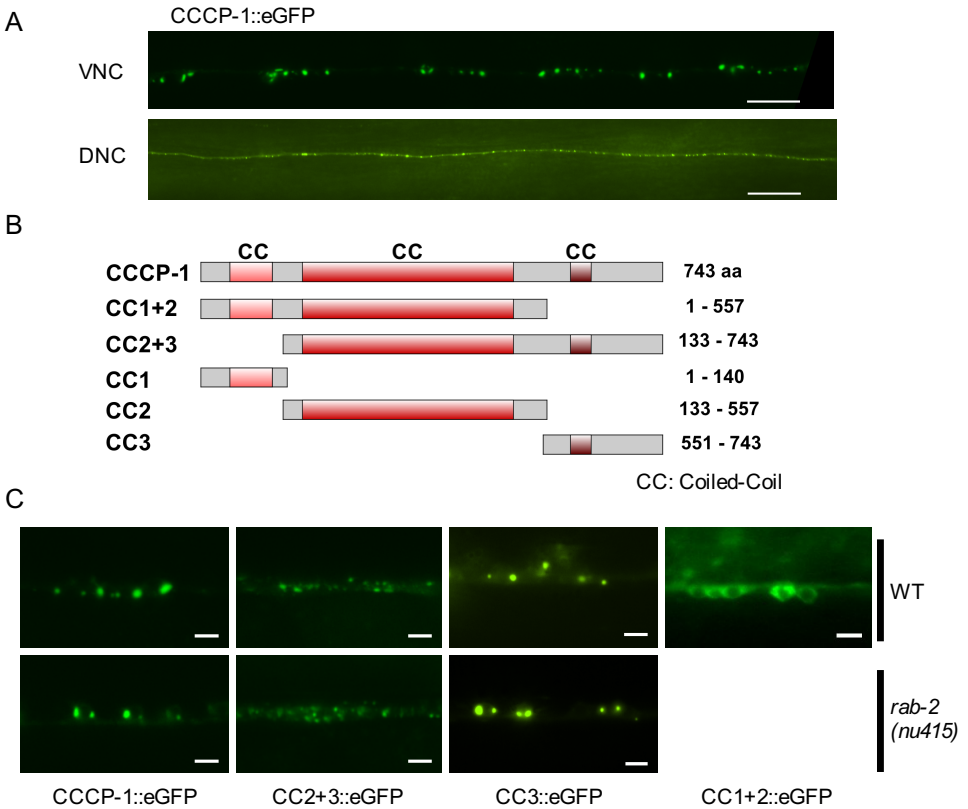

FIGURE 1. **The CC3 C-terminal domain of CCCP-1 localizes the protein.** (A) CCCP-1 localizes to perinuclear and axonal puncta. Representative images of CCCP-1::eGFP expressed under the pan-neuronal *rab-3* promoter, showing cell bodies of *C. elegans* ventral cord motor neurons (VNC) and axons of the dorsal nerve cord (DNC). Scale bar: 20 µm. (B) Domain structure of worm CCCP-1 and its different fragments. The CC1, CC2 and CC3 fragments carry the predicted coiled-coil domains. (C) CC3 is necessary and sufficient for CCCP-1 to localize, independently of RAB-2. Representative images of ventral cord motor neuron cell bodies expressing CCCP-1::eGFP or fragments, in wild type (upper panel) and *rab-2 (nu415)* mutant (lower panel) backgrounds. Scale bar: 5 µm

Figure 2

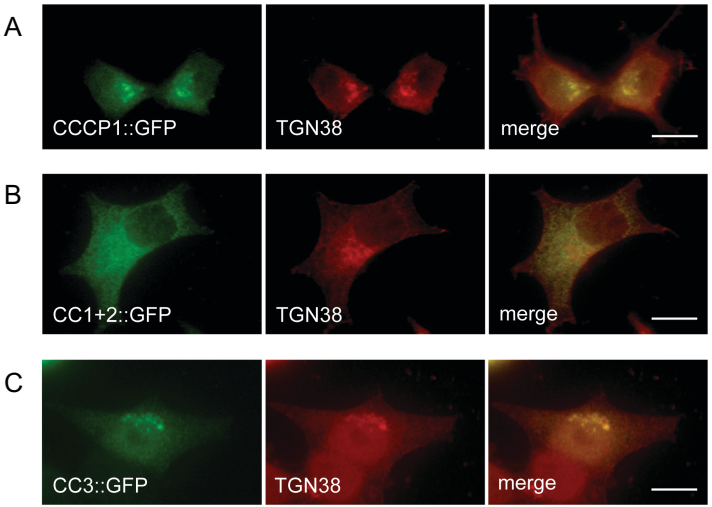

FIGURE 2. **CC3 is necessary and sufficient for localization of rat CCCP1/CCDC186 to the trans-Golgi**. (A) Representative images of 832/13 cells expressing full-length rat CCCP1::eGFP (922 amino acids) and costained for endogenous TGN38. Scale bar: 10 µm. (B) Representative images of 832/13 cells expressing CC1+2::eGFP (amino acids 1-743) and costained for endogenous TGN38. Scale bar: 10 µm. (C) Representative images of 832/13 cells expressing CC3::eGFP (amino acids 750-922) and costained for endogenous TGN38. Scale bar: 10 µm.

Figure 3

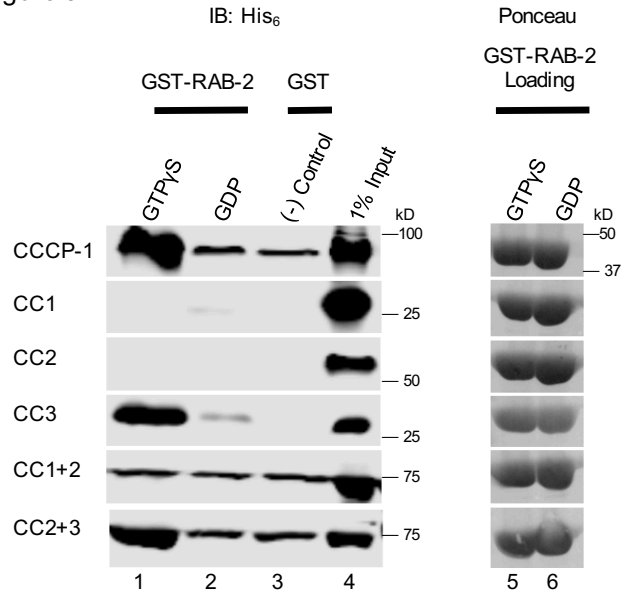

FIGURE 3. **The CC3 domain of CCCP-1 binds directly to RAB-2.** (Left) GST-pulldowns were performed using purified recombinant His_6-CCCP-1 or its fragments and GST-RAB-2 loaded with either GTPγS (lane 1) or GDP (lane 2). GST on its own was used as a negative control (lane 3). 1% of the protein input is shown in lane 4. Samples were analyzed by Western blot against the His_6 epitope tag. (Right) GST-RAB-2 loading controls visualized by Ponceau staining show that approximately equal amounts of GST-RAB-2 were used (lanes 5 and 6). IB: Immunoblot.

Figure 4

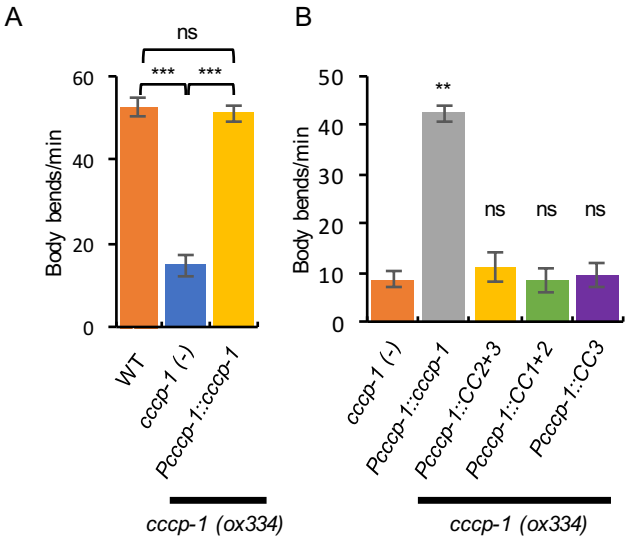

FIGURE 4. **CC3 is necessary but not sufficient for CCCP-1 function in locomotion.** (A) *cccp-1* mutant animals have slow locomotion which is rescued by a single-copy transgene of GFP-tagged CCCP-1 cDNA expressed under the *cccp-1* promoter. (***: $p < 0.001$, ns: $p > 0.05$), n=10 each. (B) The slow locomotion of *cccp-1* mutants is not rescued by expression of CC3 or other CCCP-1 fragments. (**: $p < 0.01$, ns: $p > 0.05$ compared to *cccp-1* mutant), n=10 each.

Figure 5

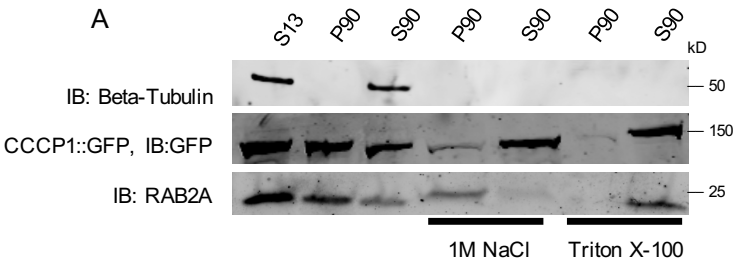
A
S13
P90
S90
P90
S90
P90
S90
kD
IB: Beta-Tubulin
CCCP1::GFP, IB:GFP
IB: RAB2A
50
150
25
1M NaCl
Triton X-100

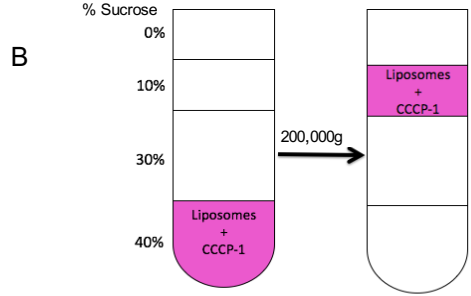
B
% Sucrose
0%
10%
30%
40%
Liposomes + CCCP-1
200,000g
Liposomes + CCCP-1

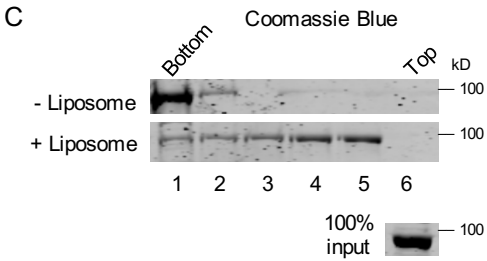
C
Coomassie Blue
Bottom
Top
kD
- Liposome
+ Liposome
100
100
1 2 3 4 5 6
100% input
100

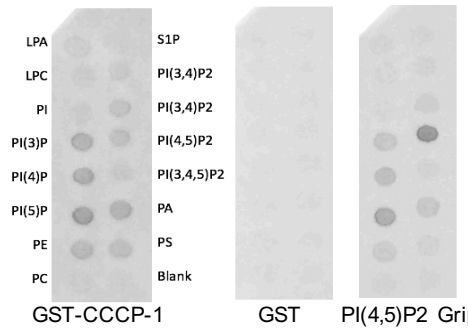
D
LPA
LPC
PI
PI(3)P
PI(4)P
PI(5)P
PE
PC
S1P
PI(3,4)P2
PI(3,4)P2
PI(4,5)P2
PI(3,4,5)P2
PA
PS
Blank
GST-CCCP-1
GST
PI(4,5)P2 Grip

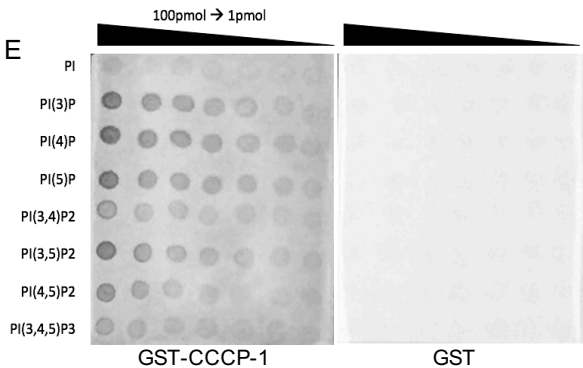
E
100pmol → 1pmol
PI
PI(3)P
PI(4)P
PI(5)P
PI(3,4)P2
PI(3,5)P2
PI(4,5)P2
PI(3,4,5)P3
GST-CCCP-1
GST

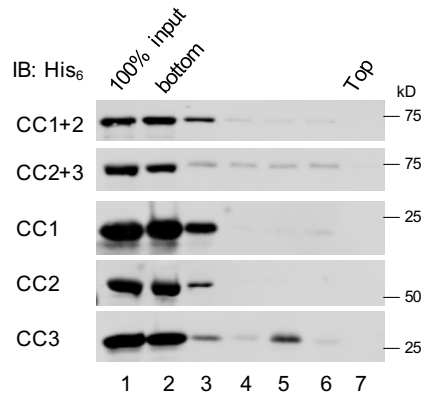
F
IB: His6
100% input
bottom
Top
kD
CC1+2
CC2+3
CC1
CC2
CC3
75
75
25
50
25
1 2 3 4 5 6 7

FIGURE 5. **CC3 binds membranes directly.** (A) Rat CCCP1/CCDC186 is a peripheral membrane protein. In insulinoma 832/13 cell fractions, rat CCCP1/CCDC186 was found primarily in the post-nuclear P90 membrane fraction and could be extracted by 1 M NaCl or Triton X-100. RAB2A associates with membranes via a lipid anchor and could be extracted by Triton X-100 but not by 1 M NaCl. Tubulin served as a control soluble protein. S13: the supernatant obtained by a 13,000g spin of the post-nuclear supernatant, containing the cytosolic proteins and proteins associated with small membrane compartments. S90, P90: supernatant and pellet fractions obtained by a 90,000g spin of the S13 fraction, containing cytosolic and membrane-associated proteins respectively. (B) Schematic of the liposome flotation assay. The CCCP-1 protein (1 μM) was incubated with Golgi-mix liposomes (1 mM lipids) containing a rhodamine-labeled lipid. The suspension was adjusted to 40% w/v sucrose and overlaid with three cushions of decreasing sucrose concentration. The tube was centrifuged for two hours at 200,000g. The efficiency of the flotation is demonstrated by observing the rhodamine-labeled lipid at the top of the tube. (C) CCCP-1 binds to membranes directly. CCCP-1 membrane-binding activity was assayed by liposome flotation. Untagged recombinant CCCP-1 was assayed in the absence (top) or presence (bottom) of "Golgi-mix" liposomes. After centrifugation, fractions were collected from the top (lane 6) to the bottom (lane 1) and analyzed by Coomassie-stained SDS-PAGE. (D) CCCP-1 binds to phosphatidylinositol lipids with a single phosphate group. Equimolar amounts of GST-CCCP-1 or GST were incubated with membranes coated with different membrane phospholipids (PIP strips). Binding activity was detected using an antibody to the GST tag. PI(4,5)P2 Grip, a GST-tagged PLC-δ1-PH domain protein, was used as a positive control. LPA: lysophosphatidic acid, LPC: lysophosphocholine, PI: phosphatidylinositol, PI(3)P: phosphatidylinositol (3) phosphate, PI(4)P: phosphatidylinositol (4) phosphate, PI(5)P: phosphatidylinositol (5) phosphate, PE: phosphatidylethanolamine, PC: phosphatidylcholine, S1P: sphingosine 1-phosphate, PI(3,4)P2: phosphatidylinositol (3,4) bisphosphate, PI(3,5)P2: phosphatidylinositol (3,5) bisphosphate, PI(4,5)P2: phosphatidylinositol (4,5) bisphosphate, PI(3,4,5)P3: phosphatidylinositol (3,4,5) trisphosphate, PA: phosphatidic acid, and PS: phosphatidylserine. (E) CCCP-1 does not show obvious binding selectivity between phosphatidylinositol lipids. Equimolar amounts of GST-CCCP-1 or GST were incubated with membranes coated with different phosphatidylinositols of decreasing concentration (PIP arrays). Binding activity was detected using an antibody to the GST tag. (F) CC3 is necessary and sufficient for CCCP-1 membrane association. Representative blots from flotation assays using "Golgi-mix" liposomes and His_6-tagged recombinant CCCP-1 fragments. After centrifugation, fractions were collected from the top (lane 7) to the bottom (lane 2) and analyzed by Western blot against the His_6 epitope tag.

Figure 6

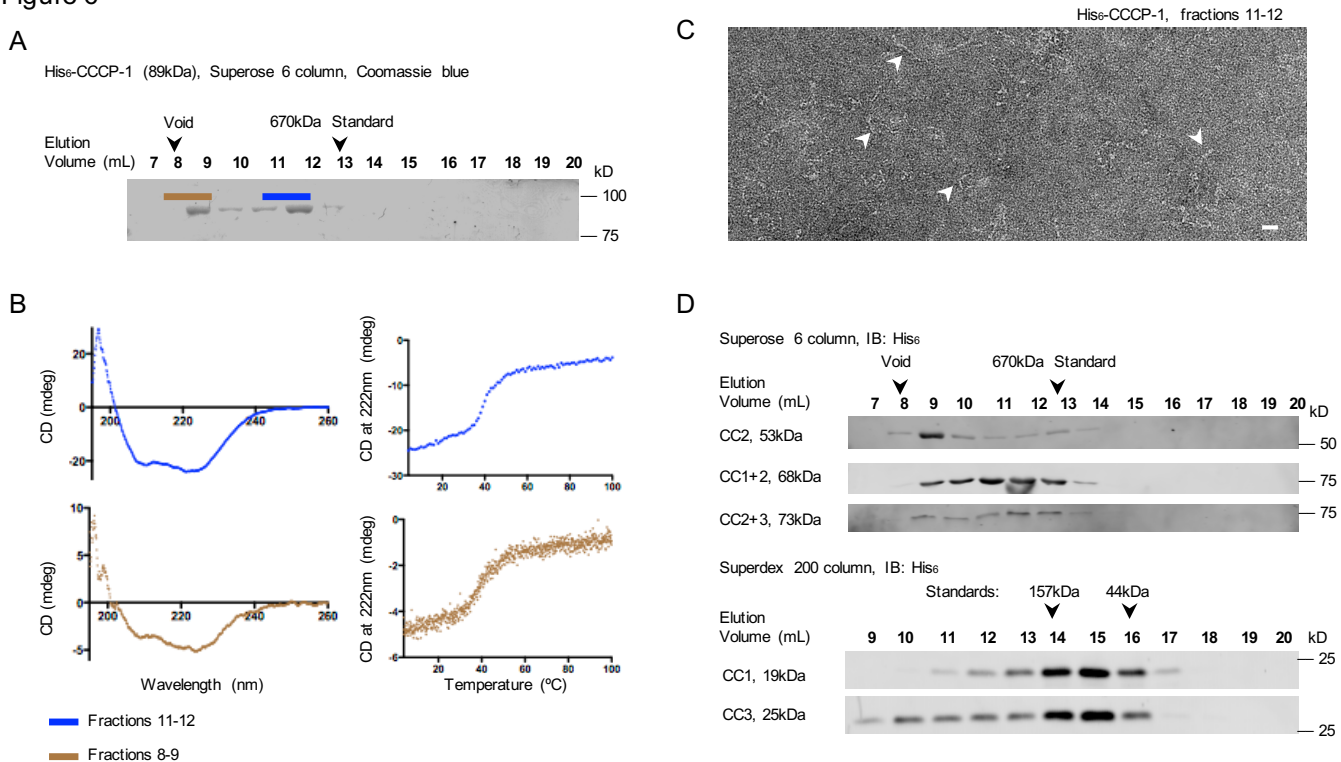

FIGURE 6. **The CCCP-1 protein is alpha-helical and forms oligomers.** (A) Recombinant CCCP-1 protein runs larger by gel filtration than its predicted molecular weight. CCCP-1 protein eluted in two peaks larger than the 670 kDa thyroglobulin standard. The brown and blue bars show the fractions collected and analyzed by CD spectroscopy (see Fig. 6B). (B) CCCP-1 is folded and composed mostly of alpha helices. Fractions eluting off the Superose 6 column (as shown in panel A) were analyzed by circular dichroism (CD) spectroscopy. (Left) Far-UV CD spectra of His_6 tagged CCCP-1: ellipticity (mdeg) was plotted as a function of wavelength (nm). (Right) Melting curve spectra: ellipticity (mdeg) was measured as a function of increasing temperature. (C) CCCP-1 forms elongated and floppy filaments. Negative-stain electron microscopy of His_6-CCCP-1. Protein eluting off a Superose 6 Column (fractions 11 and 12) was imaged by electron microscopy. White arrowheads point to the elongated flexible structures. Scale bar: 20 nm. (D) The central CC2 domain is responsible for the large apparent molecular mass of CCCP-1. Fractionation of CCCP-1 fragments by gel filtration on a Superose 6 column for large fragments (top) or Superdex 200 column for smaller fragments (bottom). 1 mL fractions were collected and analyzed by Western blot against the His_6 epitope tag. IB: immunoblot.

The Dense-Core Vesicle Maturation Protein CCCP-1 Binds both RAB-2 and Membranes through a Conserved C-terminal Coiled-coil Domain

Jérôme Cattin-Ortolá, Irini Topalidou, Annie Dosey, Alexey J. Merz and Michael Ailion

Supplemental Data

Figure S1. Alignment of the CCCP-1 protein

Figure S1

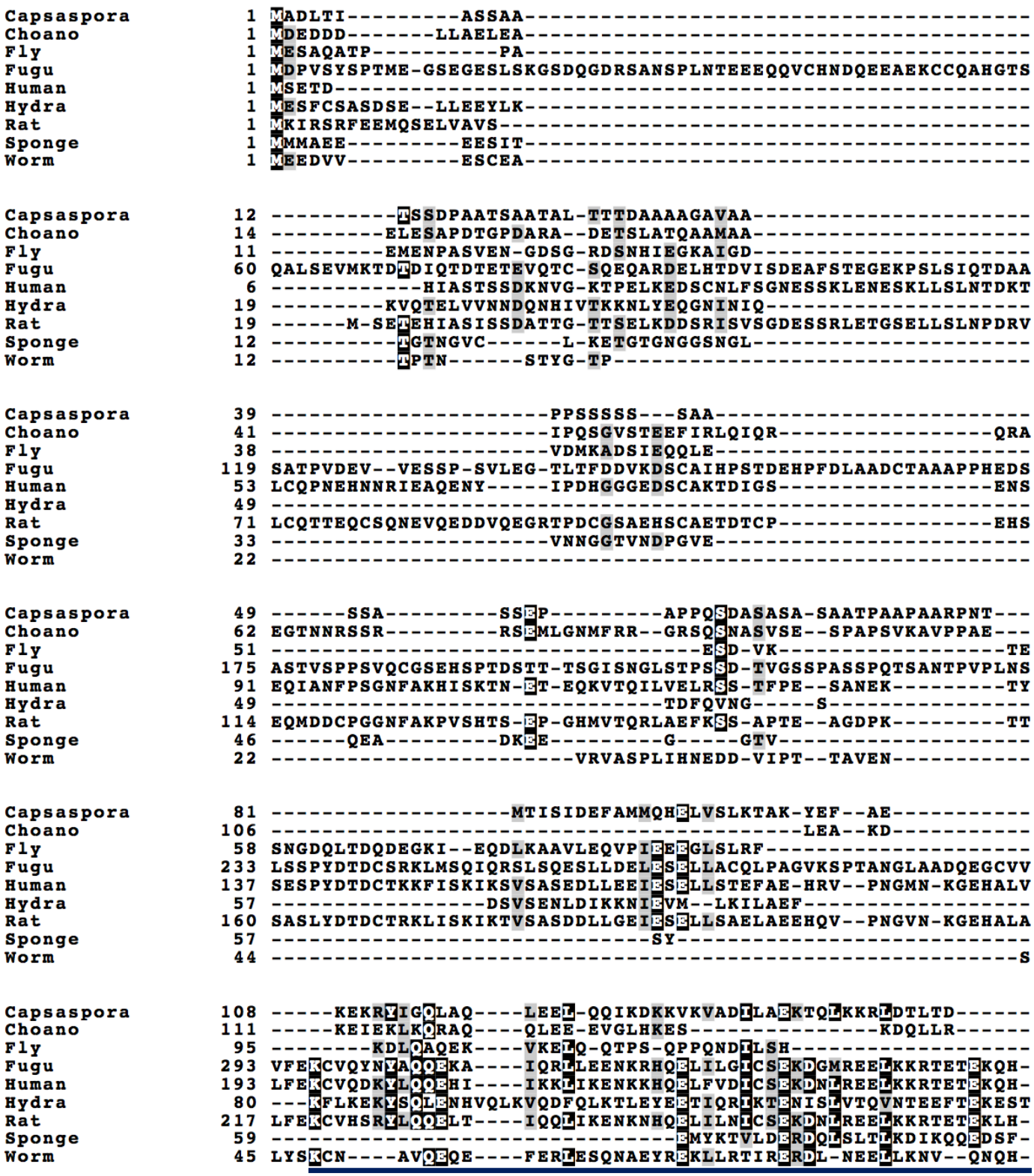

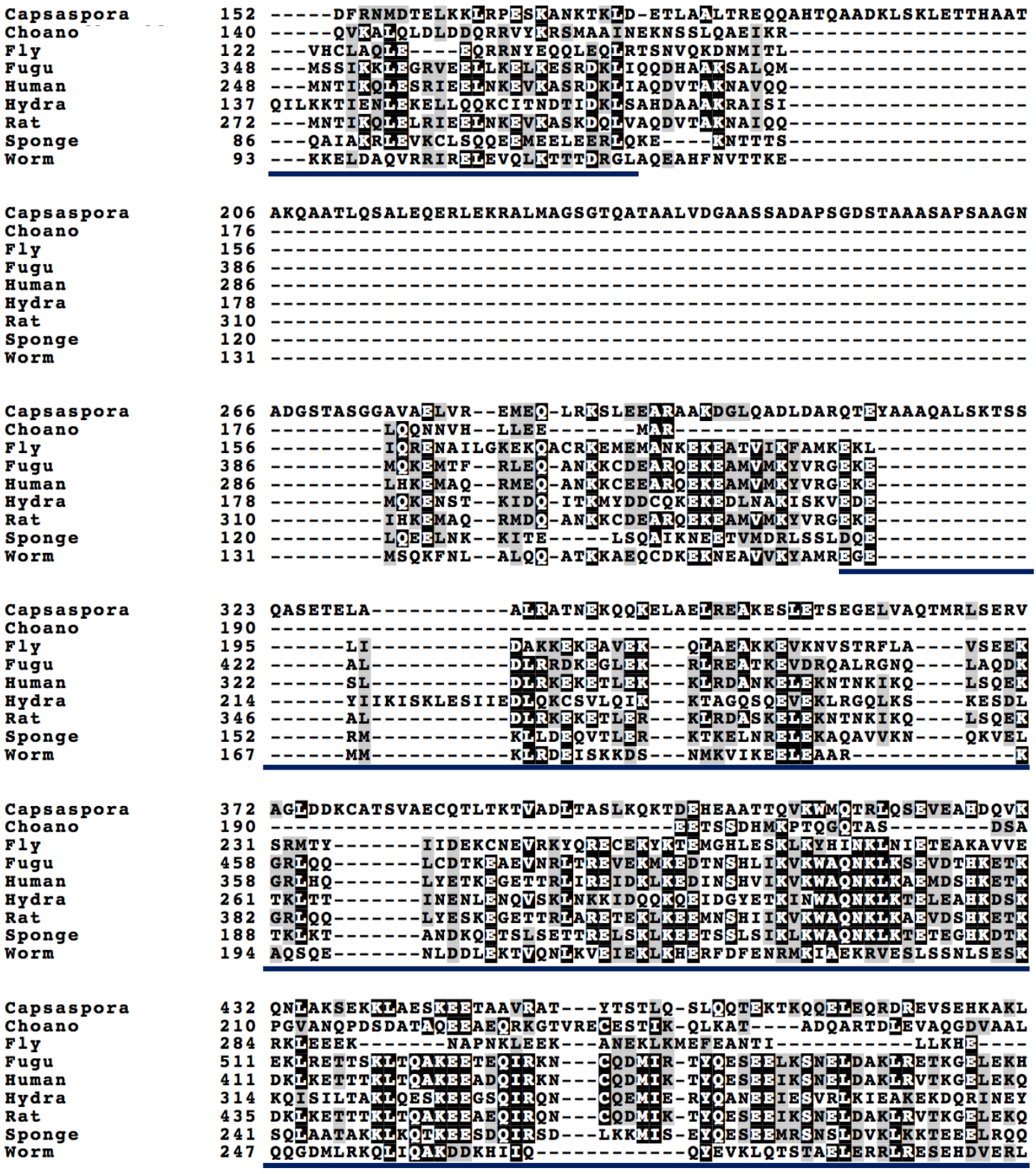

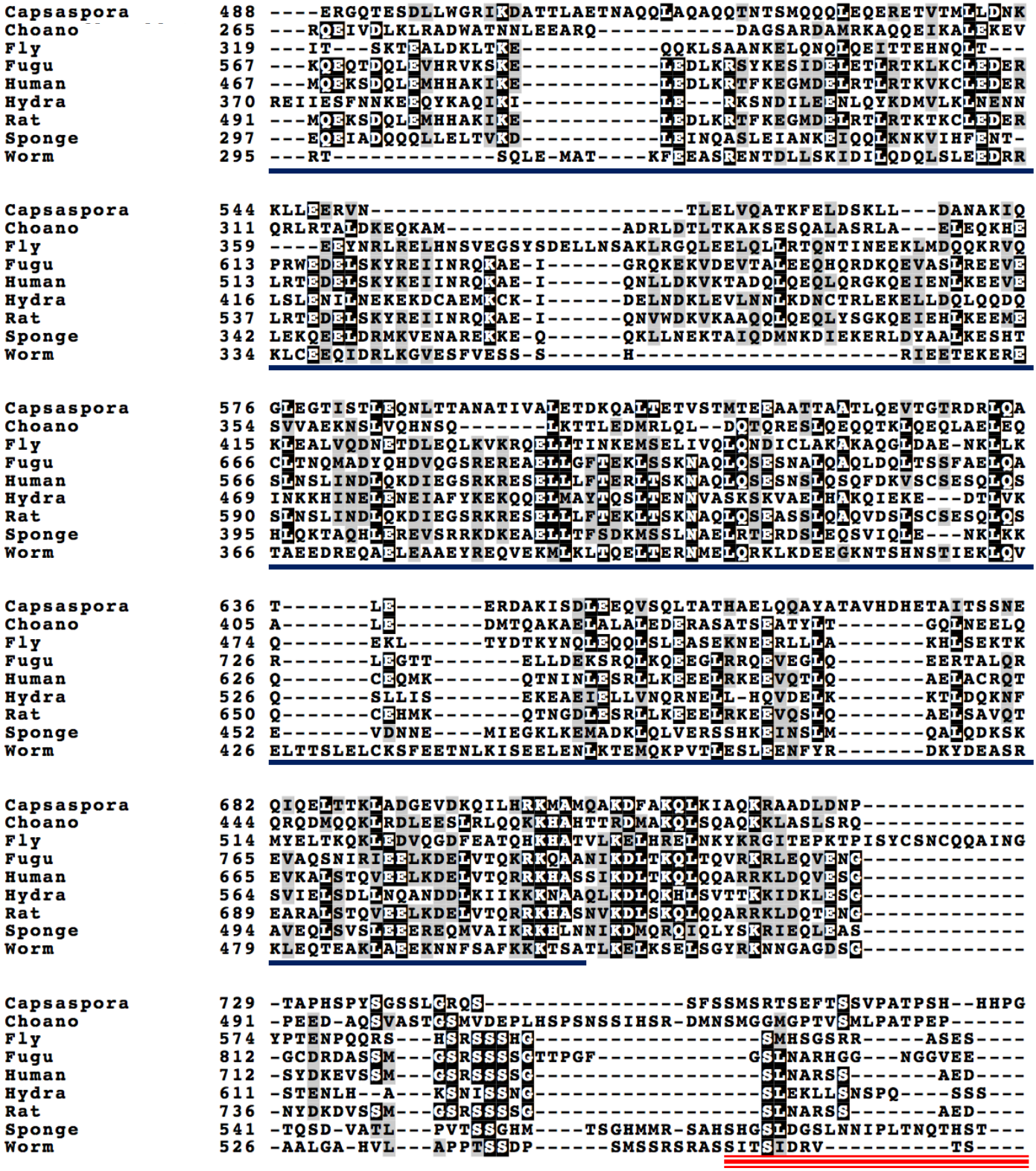

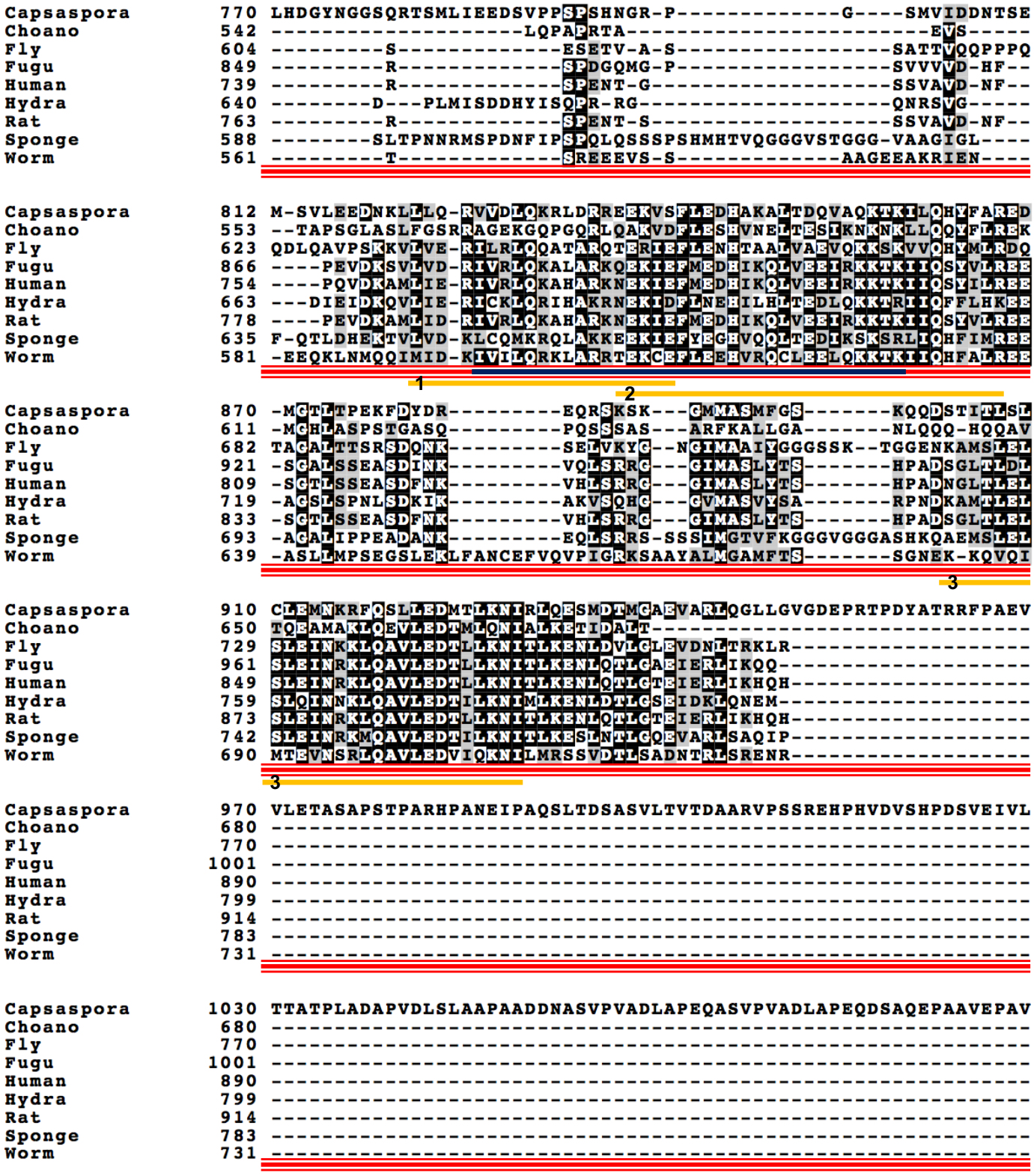

```
Capsaspora      1090 AEQAPVEQAPVEPAAVEPAAVEPAAAAPEPAAAAEQPAPVEAPALESSPAEDQPIQQADA
Choano           680 ------------------------------------------------------------
Fly              770 ------------------------------------------------------------
Fugu            1001 ------------------------------------------------------------
Human            890 ------------------------------------------------------------
Hydra            799 ------------------------------------------------------------
Rat              914 ------------------------------------------------------------
Sponge           783 ------------------------------------------------------------
Worm             731 ------------------------------------------------------------

Capsaspora      1150 PEIAPDSTIAAEPLPEQASDEAQPDANPVTDAAAESAPLPDAVPAEETTPDVPSQDE---
Choano           680 ------------------------------------------------------------
Fly              770 ----------------------------------------------------------SL---
Fugu            1001 ------------------------------------------------------------
Human            890 ----------------------------------------------------------EL---
Hydra            799 ------------------------------------------------------------
Rat              914 ----------------------------------------------------------EL---
Sponge           783 ----------------------------------------------------------K----
Worm             731 ----------------------------------------------------------LLSLS

Capsaspora      1207 -ASEDSLL
Choano           680 ------KA
Fly              772 ---EGSCK
Fugu            1001 ------RS
Human            892 -EQRTKKT
Hydra            799 ---RSSKK
Rat              916 -EQRTKKA
Sponge           784 -NTSTSNR
Worm             736 QVRTTQDN
```

CC3 fragment
Predicted Coiled-Coil domains
Amphipathic helix

FIGURE S1. **Alignment of the CCCP-1 protein.** Alignment of CCCP-1 proteins from *Capsaspora owczarzaki* (Capsaspora, CAOG_00459, accession # XP_004365330.2), *Monosiga brevicollis* (Choano, hypothetical protein, accession # XP_001745351.1), *Drosophila melanogaster* (Fly, golgin 104, accession # NP_648879.1), *Takifugu rubripes* (Fugu, Ccdc186, XP_011604585.1), *Homo sapiens* (Human, Ccdc186, accession # AAI03500.1), *Hydra vulgaris* (Hydra, Ccdc186-like, XP_012558241.1), *Rattus norvegicus* (Rat, Ccdc186, accession # KX954625), *Amphimedon queenslandica* (Sponge, Ccdc186-like, XP_011409991.1), *C. elegans* (Worm, CCCP-1b, accession # NP_499628.1). Identical residues are shaded in black and similar residues are shaded in grey. Alignment was made with T-Coffee (1), http://www.ebi.ac.uk/Tools/msa/tcoffee/, using default parameters and exhibited with BoxShade 3.21 (http://embnet.vital-it.ch/software/BOX_form.html). The coiled-coil domains of the worm protein (from SMART (2), http://smart.embl-heidelberg.de) are marked with blue bars. The CC3 domain of CCCP-1 is marked with a red bar. The presence of potential amphipathic helices in the CC3 domain was determined using the following settings in HeliQuest (3) (http://heliquest.ipmc.cnrs.fr): Helix type: α, window size: 18 amino acids, Hydrophobic moment (μH) peaks above 0.35. The predicted helices with a patch of five or more hydrophobic amino acids are numbered 1, 2 and 3. In the human ortholog, the region of helices #1 and #2 is still predicted to form amphipathic helices, but the region of helix #3 is not predicted to form an amphipathic helix.

1. C, N., Dg, H., and J, H. (2000) T-Coffee: A novel method for fast and accurate multiple sequence alignment. *J. Mol. Biol.* **302**, 205–217
2. Schultz, J., Milpetz, F., Bork, P., and Ponting, C. P. (1998) SMART, a simple modular architecture research tool: Identification of signaling domains. *Proc. Natl. Acad. Sci.* **95**, 5857–5864
3. Gautier, R., Douguet, D., Antonny, B., and Drin, G. (2008) HELIQUEST: a web server to screen sequences with specific α-helical properties. *Bioinformatics*. **24**, 2101–2102